UNLIMITED

DRA/Mar TM(MTH)91320
AUGUST 1991
Copy No. 25

DEFENCE RESEARCH AGENCY
MARITIME DIVISION
ARE Haslar, Gosport, Hants PO12 2AG

LIFT COEFFICIENT OF A RANDOMLY OSCILLATING HYDROPLANE

M J Smith

DRIC U

DRIC Y

Reports quoted are not necessarily available to members of the public or to commercial organisations.

DRA/Mar TM(MTH)91320

August 1991

LIFT COEFFICIENT OF A RANDOMLY OSCILLATING HYDROPLANE

By

M J Smith

Summary

This report describes the measurement of lift on a randomly oscillating hydroplane and makes a comparison between oscillating the hydroplane randomly or with regular sinusoidal signals together with the different methods of analysis.

ARE Haslar Gosport Hants PO12 2AG

Contents

LIFT COEFFICIENT OF A RANDOMLY OSCILLATING HYDROPLANE

By M J Smith

1. INTRODUCTION

As experiments on low aspect ratio hydroplanes (Reference 1) were to be conducted in the Circulating Water Channel (CWC), (see Figure 1) at DRA Maritime Division ARE Haslar, the opportunity was taken to include a few tests where random signals would be used to oscillate the hydroplane instead of the current practice of using regular sinusoidal signals.

This report describes both methods of analysis and compares the techniques and results. In the 'regular' experiments (Reference 1) three different aspect ratio hydroplanes were tested in several different flow speeds and a number of different oscillation frequencies. As the 'random' tests were to be performed when the regular experiments allowed, only one hydroplane aspect ratio (1.5), (see Table 1), was tested in one flow speed (2.5 m/s nominal).

For the random experiments two spectra were used, one narrow band and one broad band. Spectrum 1 was a 5 second period ITTC spectrum covering frequencies from 0.12 Hz to 0.44 Hz. Spectrum 2 was a constant energy density spectrum covering frequencies from zero to 1.2 Hz.

The investigation was carried out under entity code RE005049
Package 15 C/09.

2. EXPERIMENTAL SETUP

The hydroplane under test was mounted on a vertical shaft which passed through a gland in one of the floor panels of the CWC. The shaft was activated by a position-control servo mounted below the floor, see Figure 2. The servo rotated the shaft through angles proportional to instantaneous signal voltage produced by a signal generator for the regular tests and by spectrum synthesizer for the random tests. The spectrum synthesizer, a BBC micro computer, is identical to those which drive the wavemakers in the Haslar Ship Tanks and Manoeuvring Tank.

The shaft was strain gauged so that, as it rotated in response to the demand from the input voltage, the torque, normal and tangential force on the hydroplane could be measured. As there were problems with one of the tangential force strain gauges it was decided to only look at the normal forces.

In addition, a Laser-Doppler velocimeter was installed to measure the flow velocity immediately ahead of the hydroplane. In the regular test the instantaneous velocity measurements were used in the calculation of lift coefficient. As the time histories of velocity showed very steady readings only the average velocity as measured by the LDV was used in the calculating of lift coefficient for the random tests.

An on-line PDP11 minicomputer was used to acquire the time histories of flow velocity, demanded angle, achieved angle, lift, drag, and torque throughout the tests, and the data was subsequently analysed using a similar machine.

Figure 2 shows how the servo was assembled, and Figure 3 illustrates the disposition of the instruments in the CWC.

In this type of experiment, serious problems can arise as a result of small amounts of backlash in the oscillation mechanism. Because the rotation of the shaft reverses twice during each cycle in sinusoidal movement, it follows that the torque will also reverse twice. At the instants of torque reversal, the presence of backlash results in temporary disconnection of the hydroplane from the actuator. The motor turns, but the hydroplane shaft does not turn until the backlash has been taken up. At this point, the shaft and hydroplane must accelerate rapidly. As a result, very large transient torques occur each time the actuating torque reverses. These transients can be reduced by controlling the shaft torque, rather than its position, to respond to the demand signal; provided the comparatively small discontinuity which arises in the shaft position signal can be tolerated. For this test, however, it was decided to attempt to produce a very low backlash system because accurate position, as well as force or torque are required for most constrained model ship experiments.

The angular range and speed, and the frequency range over which the tests were to be conducted precluded the use of a direct drive from the servo motor to the hydroplane shaft. At the low angular speeds involved, 'cogging' of the motor would have resulted in discontinuous motions and torques. The traditional way of dealing with this problem was to use a fixed-speed electric motor to power a hydraulic drive consisting of a variable swash plate pump and a hydraulic motor. The effective gear ratio depends on the relative displacements of the pump and motor, and could therefore be adjusted continuously and bidirectionally by changing the swash plate angle. A small servo motor controlling the swash plate could therefore control very large amounts of power and provide continuously varying output shaft speed. Although very reliable, these machines were very noisy, inefficient, and required frequent routine maintenance.

After some investigation, a prime mover consisting of a variable speed dc servo motor and a harmonic drive reduction gearbox was chosen for this experiment. The harmonic drive can provide very high reduction ratios with low backlash and high efficiency by means of a deformable gear. It is described in Reference 2, and has proved very suitable for this type of application. The output shaft of the harmonic drive was directly coupled to the hydroplane shaft, and a toothed belt linked the shafts to a position feedback potentiometer.

A block diagram of the servo is shown in Figures 4 and 5 gives a diagram of the strain gauge positions.

3. ANALYSIS METHOD (Regular Experiments)

The servo controlling the hydroplane was fed with a sinusoidal signal of fixed frequency and amplitude. Time histories of normal and tangential forces and achieved angular displacement were acquired for a range of frequencies and amplitudes.

By use of a least squares method the phase, relative to a fixed arbitrary reference point, and average frequency were found for each time history. As the reference point is the same for each time history the phase of the

output relative to the input can be found by subtracting one phase from the other. The average angular displacement was found by taking the average peak to trough value of each time history.

Time histories of lift were calculated from the time histories of normal and tangential forces using the following expression:

$$L = N \cos(\alpha) + T \cos(\alpha)$$

where

L is lift
N is normal force
T is tangential force
α is angular displacement

From the time histories of lift and flow velocity the lift coefficient C_L can be calculated by using:

$$C_L = \frac{L}{0.5\rho\, U^2 A}$$

where

ρ is the density of water ($10^3 kg/m^3$)
U is water flow speed
A is the area of the hydroplane

A value for the lift coefficient for each frequency and amplitude combination was computed by taking the average peak to trough value in each time history.

4. ANALYSIS METHOD (Random Experiments)

Time histories of normal and tangential forces of a randomly oscillating hydroplane were acquired using a PDP11 minicomputer. Also acquired were time histories of achieved hydroplane angle, relative to the water flow direction.

Time histories of lift and lift coefficient were calculated in the same way as for the regular experimental data. The achieved angle used was the instantaneous position corresponding to the simultaneous force measurements. From these time histories a frequency response function $H(\omega)$ was calculated.

In a simple noise free measurement of a linear system the frequency response function is the ratio of the Fourier transform of the response time history to the simultaneously measured Fourier transform of the input time history ie:

$$H(\omega) = \frac{Y(\omega)}{X(\omega)} \qquad (1)$$

In this analysis $X(\dot{\omega})$ would be the Fourier transform of the achieved hydroplane angle and $Y(\dot{\omega})$ would be the Fourier transform of lift coefficient.

The above equation (1) is only valid for the idealised case where both input and response are deterministic and noise free.

A signal classed as deterministic is one where the physical quantity being measured can be described explicitly in terms of mathematical relationships and therefore it is likely we can regard the derived signal in the same way.

In this experiment as the input signal is random, that is, we will not be able to predict precisely its value at any given future instant in time, and noise free conditions are never achieved in the experimental environment, the fundamental definition must be modified such that the analysis proceeds in terms of statistical values from which a deterministic relationship may be obtained.

This modification can be achieved by taking the ratio of the auto spectrum of the response time history (lift coefficient) to the auto spectrum of the input time history (hydroplane angle).

Unfortunately the method does not calculate any phase information. Also the measurement of the normal and tangential forces, and hence the auto spectra, will be noisy so that even after averaging, the frequency response function can be inaccurate.

A better relationship is given by multiplying the numerator and the denominator of equation (1) by the complex conjugate of the input Fourier transform, thus:

$$H(\omega) = \frac{Y(\omega)\ X^*(\omega)}{X(\omega)\ X^*(\omega)} = \frac{G_{XY}(\omega)}{G_X(\omega)}$$

where

$G_{XY}(\omega)$ is the cross spectrum of input (X) and output (Y).

$G_X(\omega)$ is the auto spectrum of the input (X).

* denotes complex conjugate.

The frequency response function will be in the complex form a + jb. To put this information in a more useful form we must calculate the modulus and phase of this response function as follows:

$$\text{modulus} = \sqrt{a^2 + b^2}$$

$$\text{phase} = \tan^{-1}(b/a)$$

5. DISCUSSION OF RESULTS

Figure 6 gives the ASD for spectrum 1 together with the resulting lift coefficient ASD. Figure 7 gives the same comparison for spectrum 2.

Figure 8 shows a comparison of the narrow band and broad band frequency response function amplitude whilst Figure 9 gives a similar comparison for the phase part of the response functions. As can be seen from these figures there is virtually no difference between the two sets of measurements. Figures 10 and 11 gives graphs of achieved hydroplane angle versus lift coefficient C_L, each dot represents one of the 4096 measurements taken during the measurement of hydroplane response to spectrum 1 and spectrum 2 respectively.

Figures 12 and 13 show comparisons, for amplitude and phase respectively, between the broad band (random input) frequency response and individual data points calculated from the regular input experiments. In Figure 12 most of the regular input data points compare very favourably with the random response curve. The few points which are below the random response curve are from the regular tests where the demanded peak to trough angular displacement was ± 40 degrees. From observations it would appear that the servo could not produce a sinusoidal change of position at this angular displacement, this would tend to make the lift response non-linear and hence invalidate the calculation of lift coefficient frequency response function. A second and more likely explanation for this discrepancy is that the lift response itself is non-linear at large angles, and this is likely to be worse at low frequencies. The most probable cause of this non-linearity is stall. There was some evidence of stall at large angles in the regular experiments, however further work is required before a firm conclusion can be drawn.

Figure 14 shows a graph of lift coefficient versus steady-state hydroplane angle. Also plotted on this figure are points from the random tests where the instantaneous values of both angular velocity and angular acceleration were zero (points from both spectra). These 'dynamic' values compare favourably with the steady-state results. It should be noted that the steady-state results were obtained from over twenty tests whereas the 'dynamic' values required only one test. The 'dynamic' values only cover a small angular range; however this range can be increased. This is discussed later on in the conclusion.

In Reference 1 Ward and Lloyd give the following formula as a method for calculation of lift coefficient if angular displacement, velocity and acceleration are known:

$$C_L = a\ddot{\alpha} + b\dot{\alpha} + c\alpha$$

where

α is angular displacement (deg)

$\dot{\alpha}$ is angular velocity (deg/sec)

$\ddot{\alpha}$ is angular acceleration (deg/sec^2)

The constants 'a', 'b' and 'c' were calculated from the regular data using a least squares method. Figure 15 gives time histories of lift coefficient produced from the random tests and a calculated time histories produced from the measured angular displacement time history and the constants

calculated by Ward and Lloyd (see Table 2). It can be seen from this figure that the calculated time history almost exactly matches the measured one.

Figures 16 and 17 show a graph of lift coefficient versus angle for all points in the random record where the angular velocity and the angular acceleration are both zero. Unlike the regular method, these data were obtained without the need to perform a separate test.

Figures 18 and 19 show a graph of lift coefficient against achieved hydroplane angle for all points in the random record where the angular velocity was zero. The lack of scatter suggests that the angular acceleration has little effect on the lift.

Figures 20 and 21 show a similar graph to that given in Figure 18 and 19, but this time the points plotted are where the angular acceleration is zero. The data appears to have a similar slope to that of the zero velocity points but shows a significant amount of scatter indicating that the angular velocity of the hydroplane has a marked effect on the lift, although it could also be partly due to backlash in the servo mechanism.

It is possible to obtain data points with zero velocity and non-zero hydroplane angle from the regular tests but these would always be at peak values of angle. In the regular tests, data points with zero acceleration would always occur at zero hydroplane angle and so would reveal little information.

To calculate the constants 'a', 'b' and 'c', for the formula produced by Ward and Lloyd (Reference 1), using the random test data, the time histories of angular displacement were differentiated once with respect to time to obtain angular velocity and twice to obtain angular acceleration. Then taking an arbitrary limit of ± 2 per cent of the peak value, the velocity and acceleration time histories were scanned and any points falling within the limit were treated as zero velocity and zero acceleration respectively.

The constant 'c' can be calculated from the slope of curve given in Figures 16 and 17 where the angular velocity and acceleration is zero and hence:

$$C_L = c\alpha$$

The slope of this curve was calculated as 0.03 per degree for both graphs whereas the value of 'c' calculated from the regular tests was 0.034 per degree. The numbers are similar.

For constants 'a' and 'b' the following formulae were derived:
when angular velocity is zero

$$a = \frac{C_L - c\alpha}{\dot{\alpha}} \ sec^2/deg$$

and when angular acceleration is zero

$$b = \frac{C_L - c\alpha}{\dot{\alpha}} \ sec/deg$$

Figures 22 and 23 give a graph of 'b' for all data points where the angular acceleration was zero, for spectrum 1 and spectrum 2 respectively. Figures 24 and 25 show a graph of 'a' when the angular velocity was zero. An average of these values was taken to give the constants 'a' and 'b', these values are given in Table 2. From this table it can be seen that the constant 'b' obtained from spectrum 2 compares well with the constant derived from the 'regular' tests. The value obtained from spectrum 1 does not compare as well but is of a similar magnitude. The values for the constant 'a' from both spectra do not compare well but acceleration has little effect on the lift coefficient and the fact that the values are relatively small seems to bear this out.

Figures 26 and 27 give a comparison of measured and calculated Lift Coefficient for spectra 1 and 2 respectively using the constants calculated from the random data. In both graphs the measured and calculated time histories compare favourably.

Figure 28 gives a comparison of lift coefficient predicted by using both sets of constants with a normalised time history of angle of attack. It was necessary to normalise the time history because at the position of the hydroplane the flow was not parallel to the sides of the CWC and therefore indicated zero angle for the hydroplane did not correspond to the angle when lift coefficient was zero. From the graph it can be seen that the predicted lift coefficient time histories do not differ significantly.

6. CONCLUSIONS AND FUTURE WORK

a. Experimentation

From these results it can be seen that measurement of lift coefficient and other similar quantities on constrained models can be conducted more quickly and efficiently using random signals. In this example the random signal method required ten minutes of experiments and a couple of hours analysis, compared to several days of experiments and about a week of analysis for the regular signal experiments. It has been shown that the random tests gave a greater range of data than the regular tests, and were able to measure some quantities, such as lift at zero acceleration and non-zero angular displacement, which were not available from the regular tests. For these reasons, an investigation into the feasibility of constructing a planar motion mechanism capable of being excited with random signals should be considered.

b. Analysis Method

Initially, to test the random method, the points where angular velocity and angular acceleration were zero were found by scanning the appropriate file to detect any points that fell within a set limit. A better method would be to interpolate each angular velocity and angular acceleration record to obtain actual zero velocity and acceleration and then find the corresponding points in the lift coefficient time histories. This would not only give more data points and a better spread of data, but would tend to reduce the scatter thereby improving the accuracy of calculation when deriving the constants 'a', 'b' and 'c'. Although the constant 'a' produced by each method did not compare favourably they are relatively small in magnitude in comparison with the constants 'b' and 'c' indicating acceleration has little effect on lift coefficient. This difference is therefore not considered significant.

In applying the transfer function measured by this method it should be remembered that a transfer function is a linearised or 'small signal' representation of system behaviour, it will not accurately predict the behaviour of the hydroplane at large angles, for example when stalled.

c. Excitation

The spectra used as input to the system were chosen somewhat arbitrarily. A more careful choice of spectra would be also likely to add to the accuracy of the method.

7. ACKNOWLEDGEMENTS

The author would like to acknowledge the help and assistance of Mr B Ward for his permission to extend his experiments and for access to experimental data used in his report. The author would also like to thank Mr S P Miles for his invaluable assistance in the preparation of the figures.

REFERENCES

1. Ward B, Lloyd A R J M. Experiments on Low Aspect Ratio Hydroplane to Measure Lift under Static and Dynamic Conditions. ARE TM(UHR)90306, March 1990. UK UNCLASSIFIED.

2. Harmonic Drive Ltd, Myrtle Lane, Billingshurst, West Sussex, RH14 9SG. Harmonic Drive Gears.

3. Beauchamp K G. Signal Processing, using Analogue and Digital Techniques.

4. Wallace R, Gabi B S Dr and Tomlinson M A. Basic Signal Processing (Cranfield Institute of Technology).

5. Fryer D K. Waves in Ship Tanks Part 2, Experiment Techniques in Random Waves. ARE TR89310, July 1989. UK UNCLASSIFIED.

Table 1

Hydroplane Number	2
Serial Number	45218
Hydroplane Area	0.0507 m^2
Aspect Ratio	1 : 1.5

Table 2

	a sec^2/deg	b sec/deg	c deg^{-1}
Regular	0.000082	0.0023	0.034
Spectrum 1	0.0011	0.0055	0.03
Spectrum 2	-0.00061	0.0026	0.03

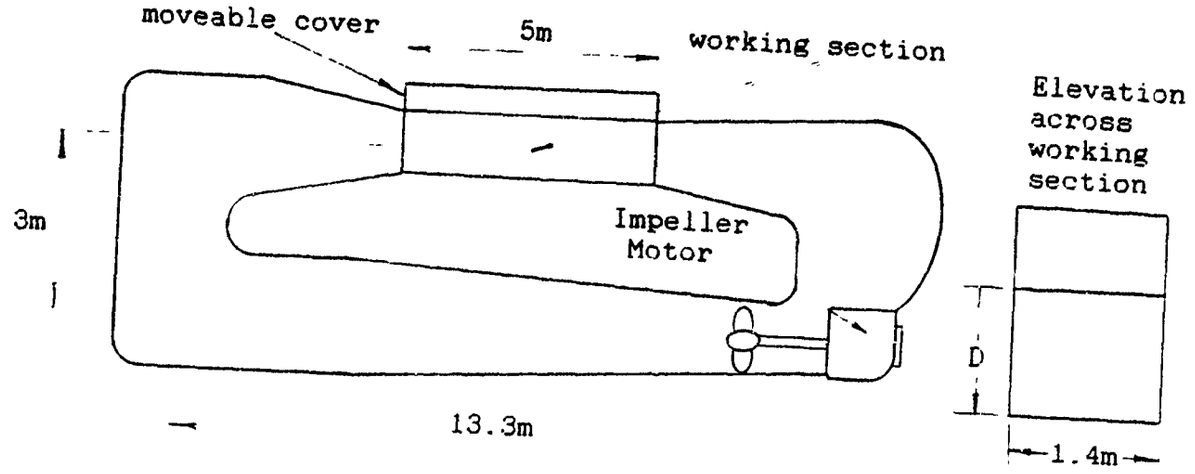

D variable between 0.15m and 0.84m

Description of facility:	vertical plane free surface circulating water channel
Type of drive system:	toothed belt driven impeller from one of two motors
Total motor power:	large motor 75kW small motor 1.5kW
Working section max. velocity:	5.5 metres/sec
Max and min ABS pressures:	100 kn/m² 40 kn/m²
Mounting of models:	models can be mounted to to suit the requirements of each experiment

FIG 1 THE CIRCULATING WATER CHANNEL AT A.R.E.(HASLAR)

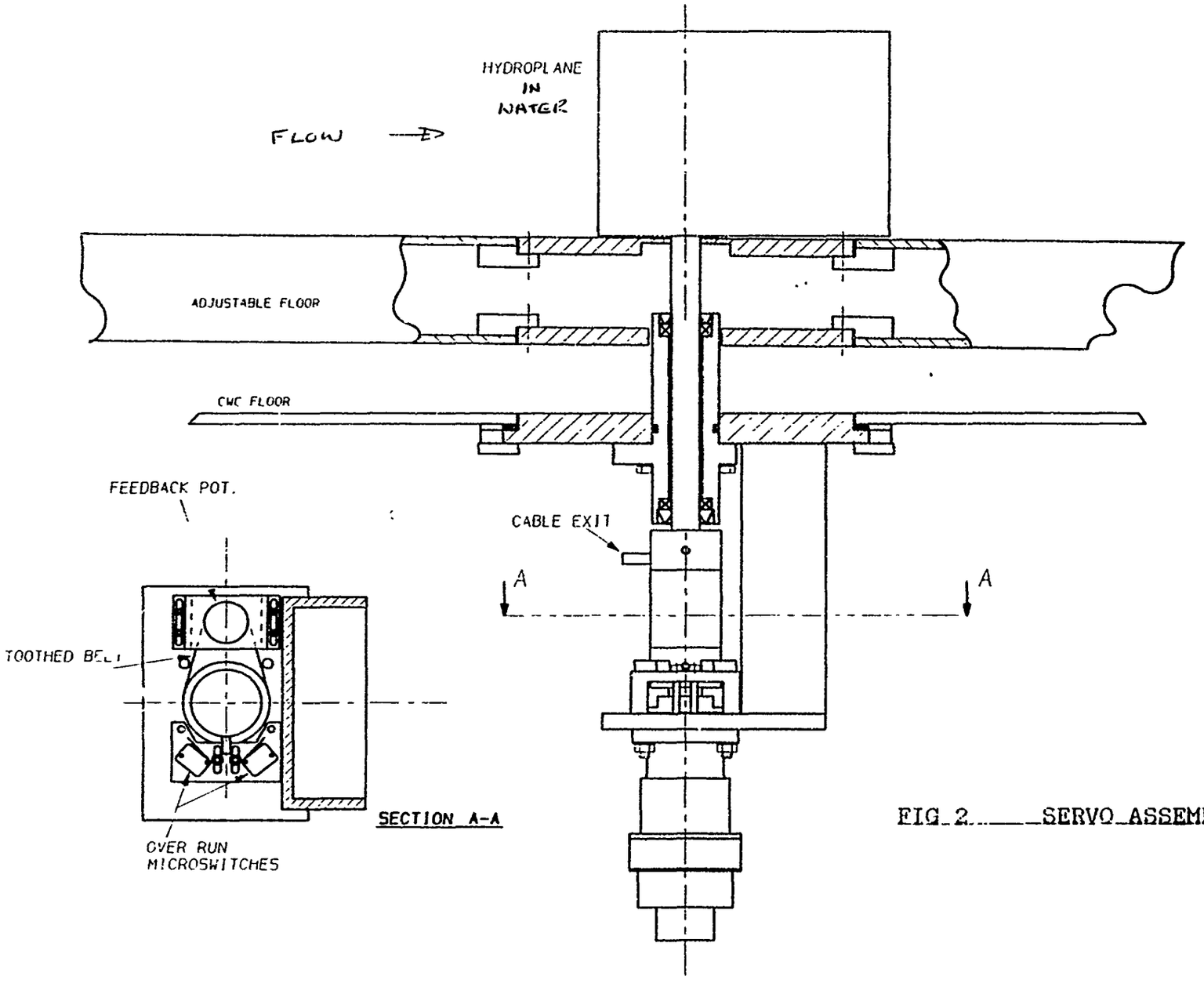

FIG. 2 SERVO ASSEMBLY

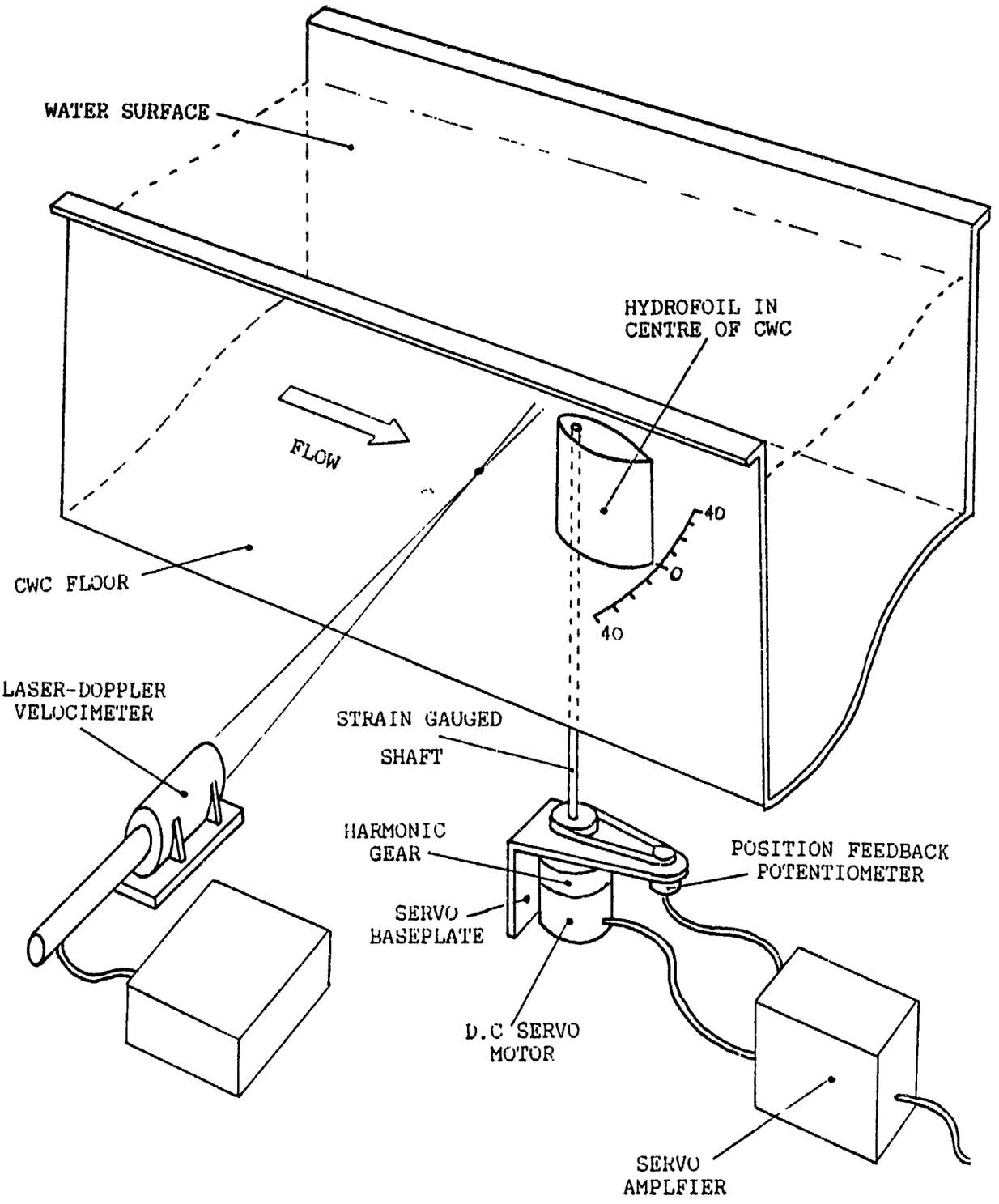

FIG 3 EXPERIMENT HARDWARE.

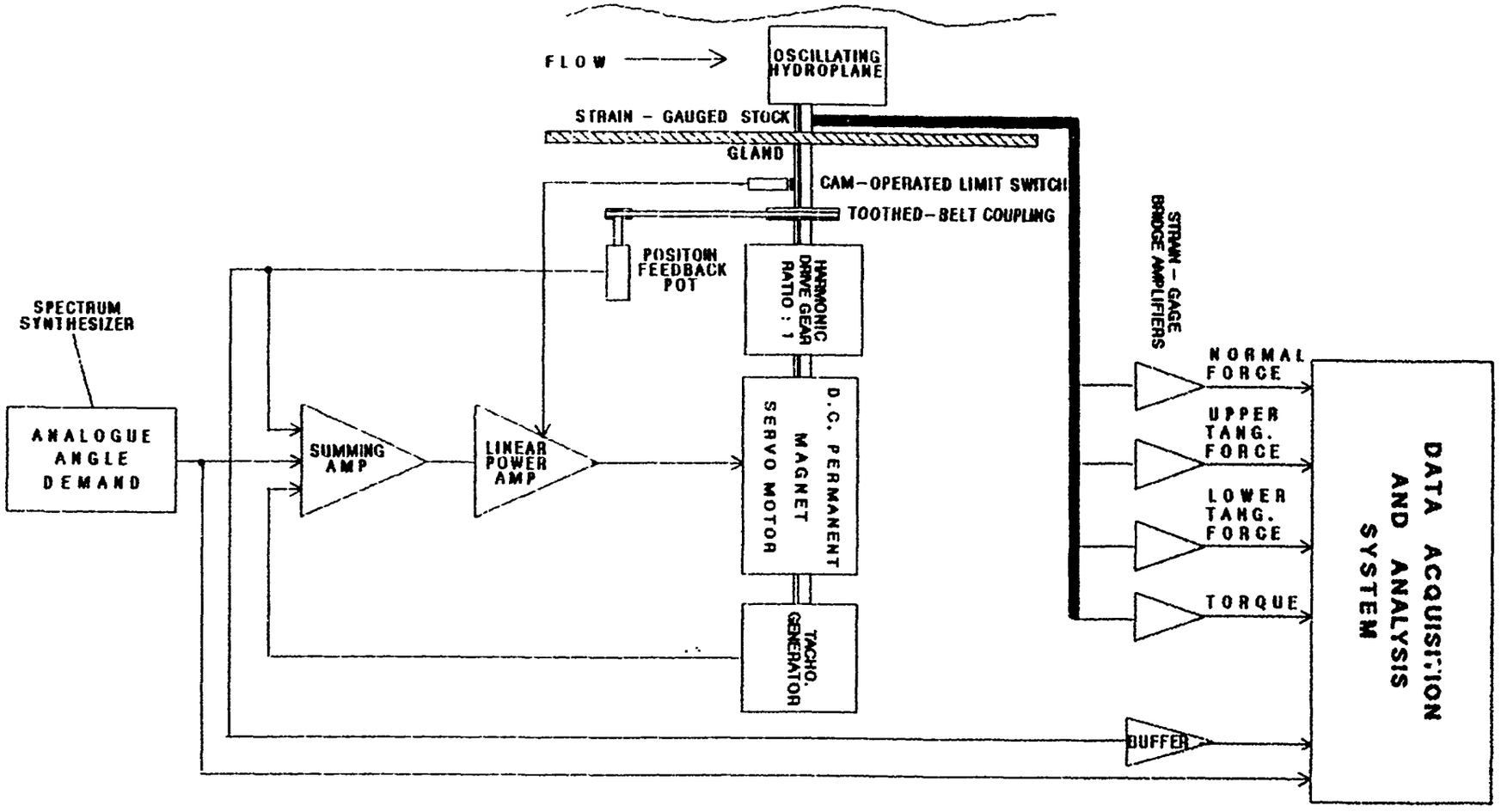

FIG 4 BLOCK DIAGRAM OF SERVO.

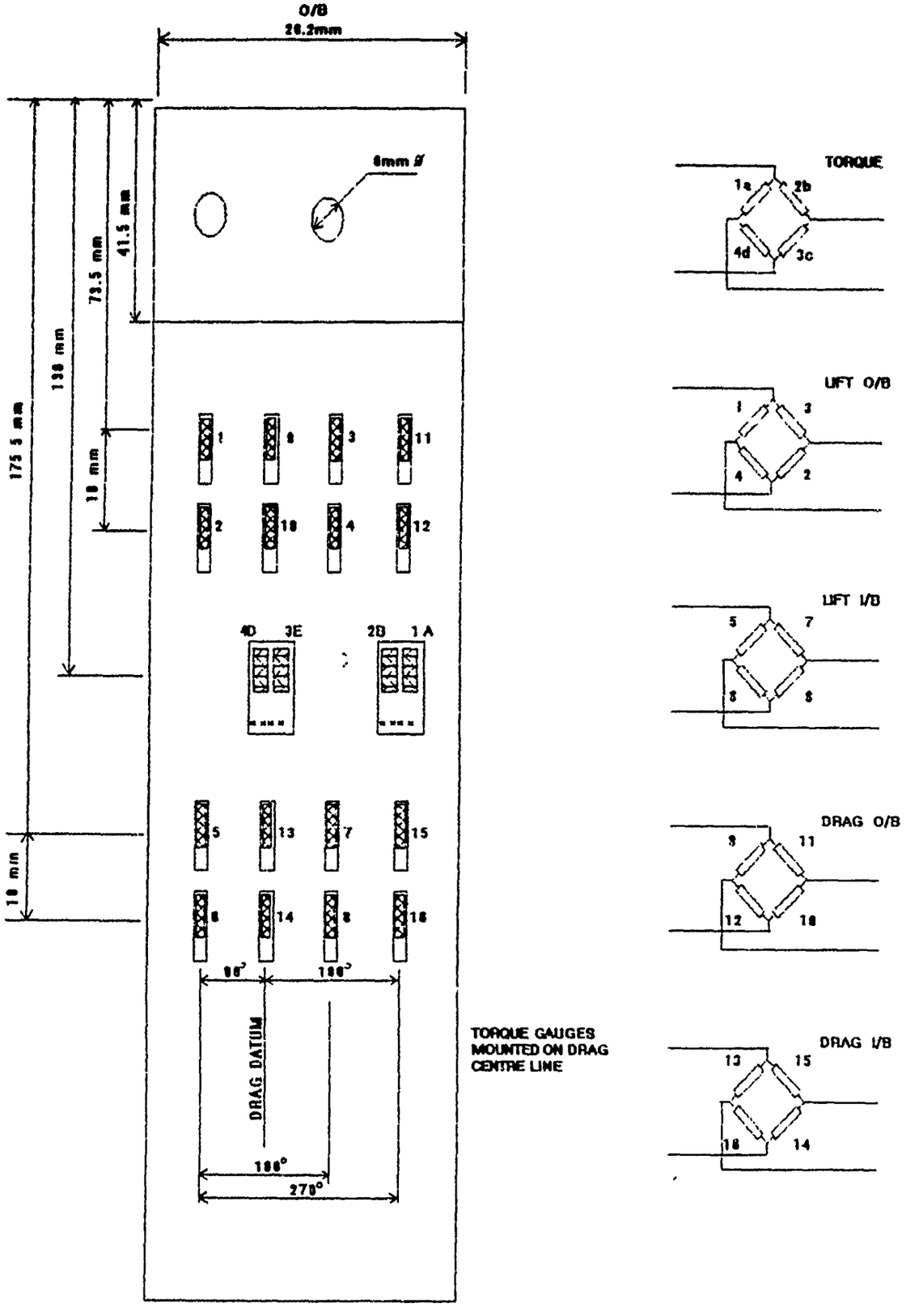

DEVELOPMENT OF CLYINDRICAL STOCK

FIG 5 DIAGRAM OF GAUGE POSITIONS

Input and Output Spectra (Spectrum 1)

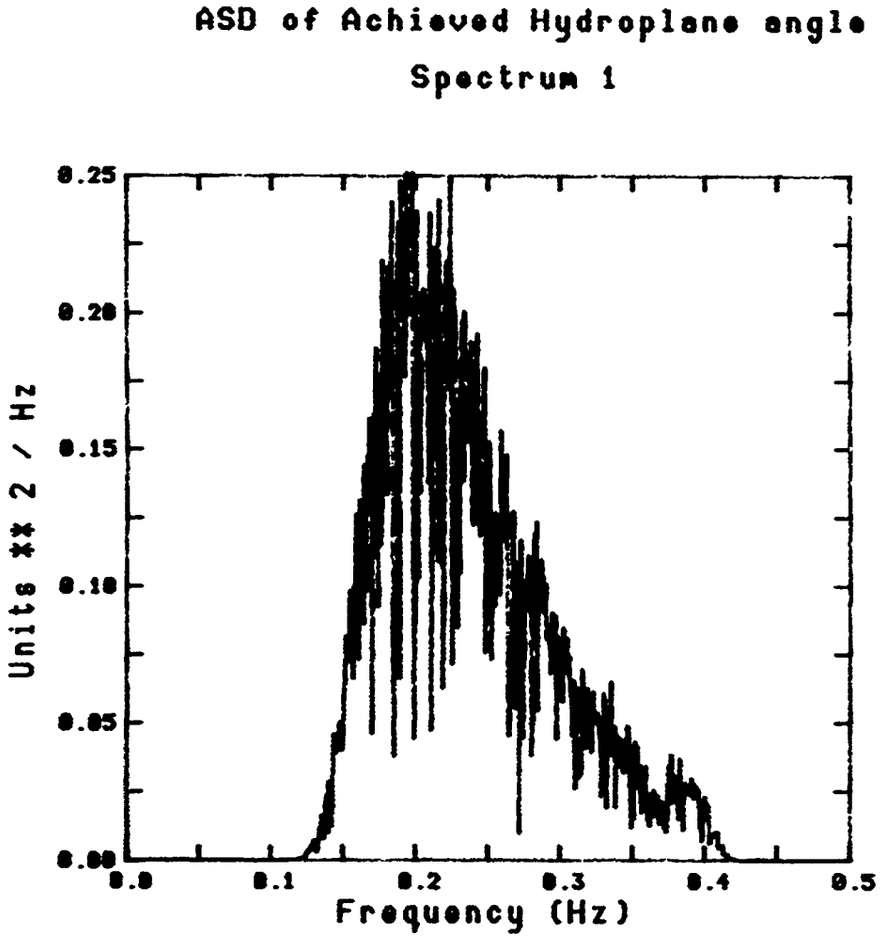

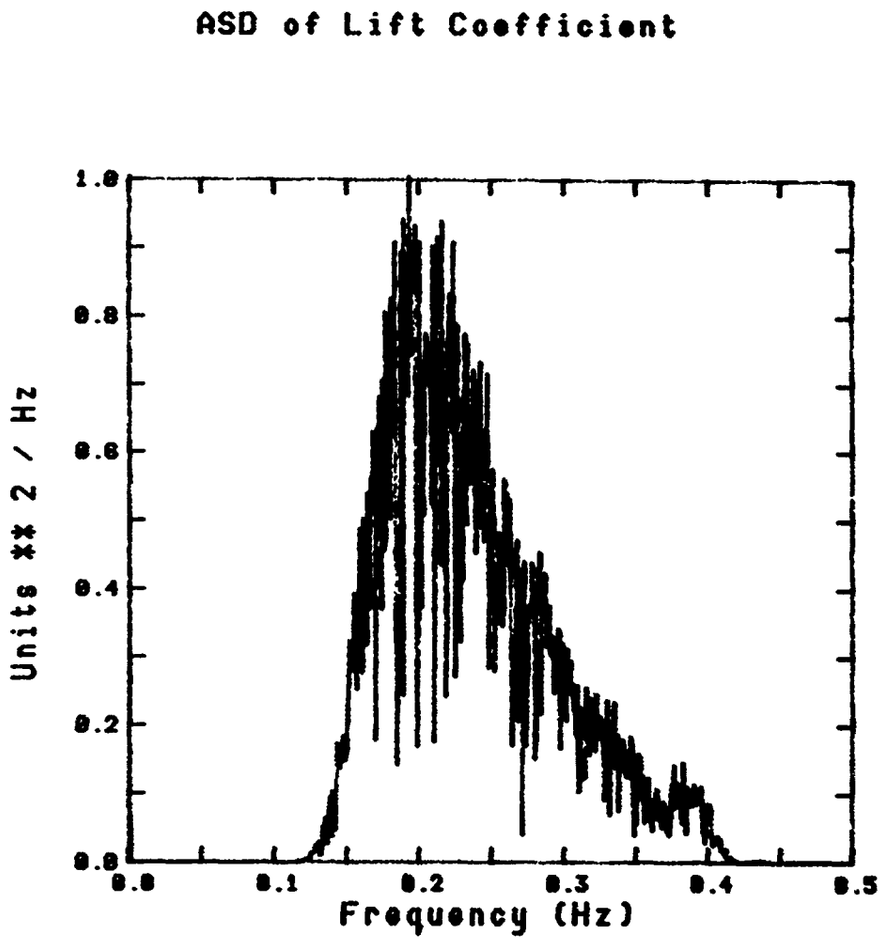

Figure 6

Input and Output Spectra (Spectrum 2)

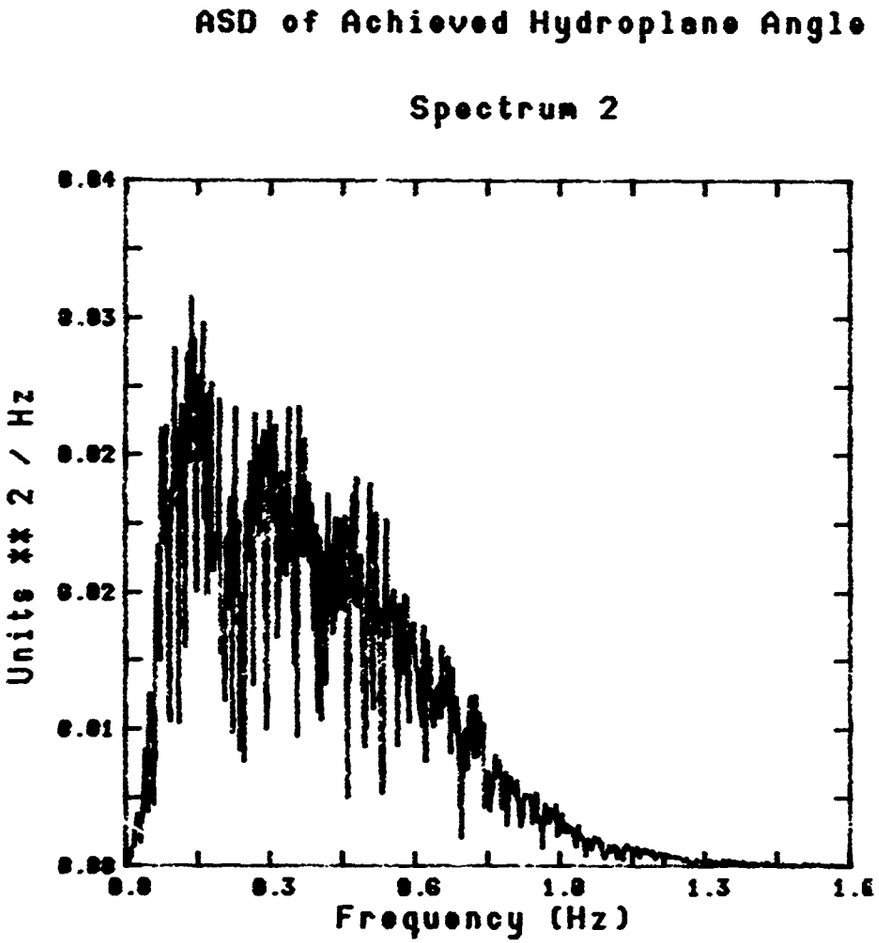

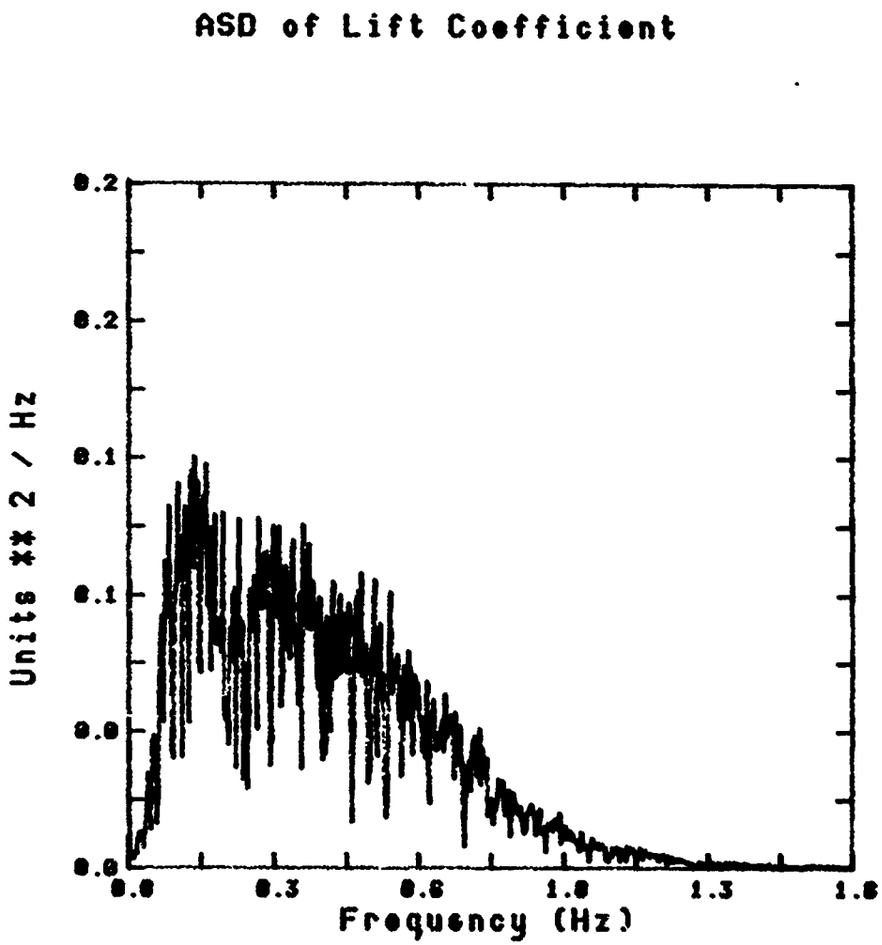

Figure 7

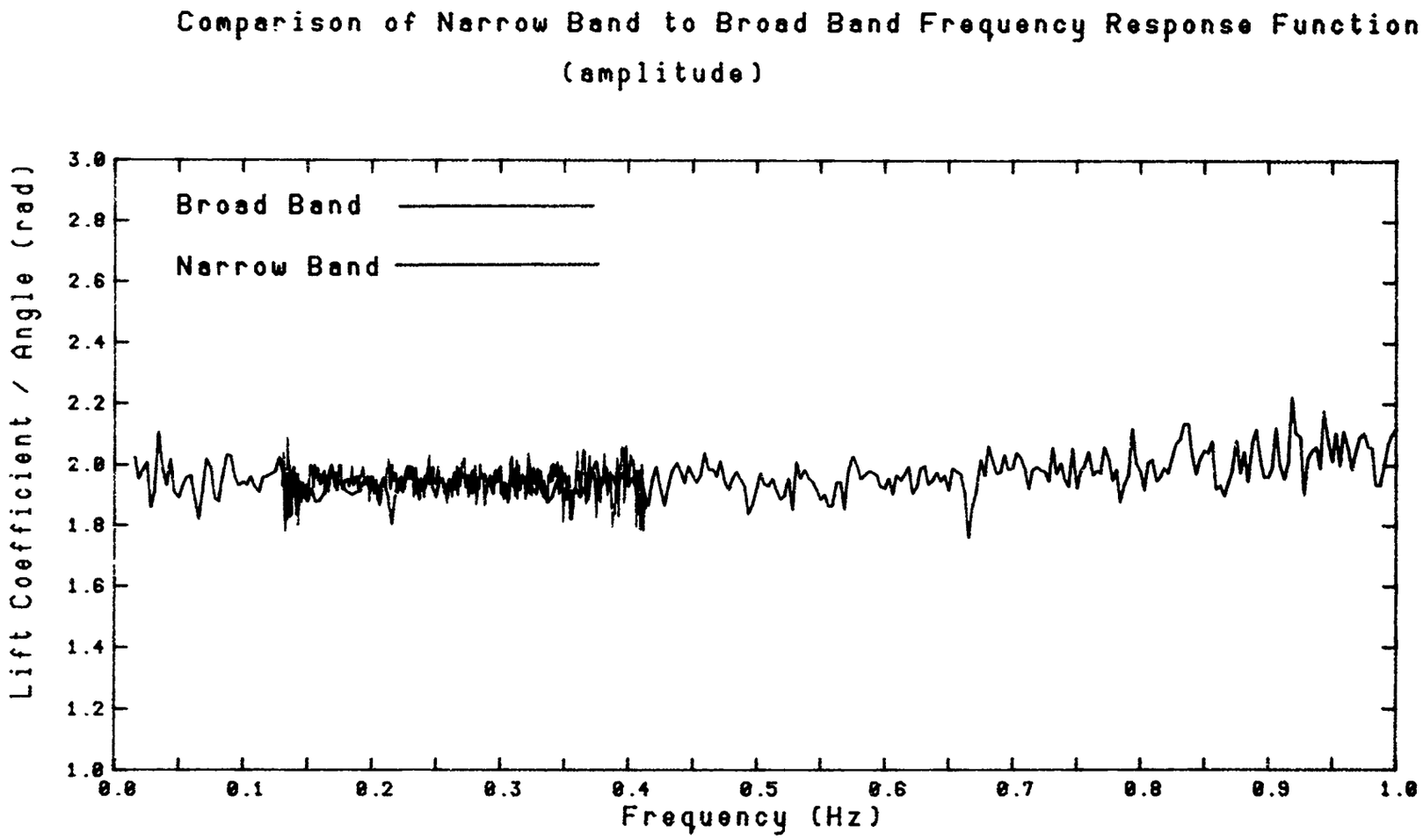
Comparison of Narrow Band to Broad Band Frequency Response Function
(amplitude)
Broad Band
Narrow Band
Lift Coefficient / Angle (rad)
3.0
2.8
2.6
2.4
2.2
2.0
1.8
1.6
1.4
1.2
1.0
0.0
0.1
0.2
0.3
0.4
0.5
0.6
0.7
0.8
0.9
1.0
Frequency (Hz)

Figure 8

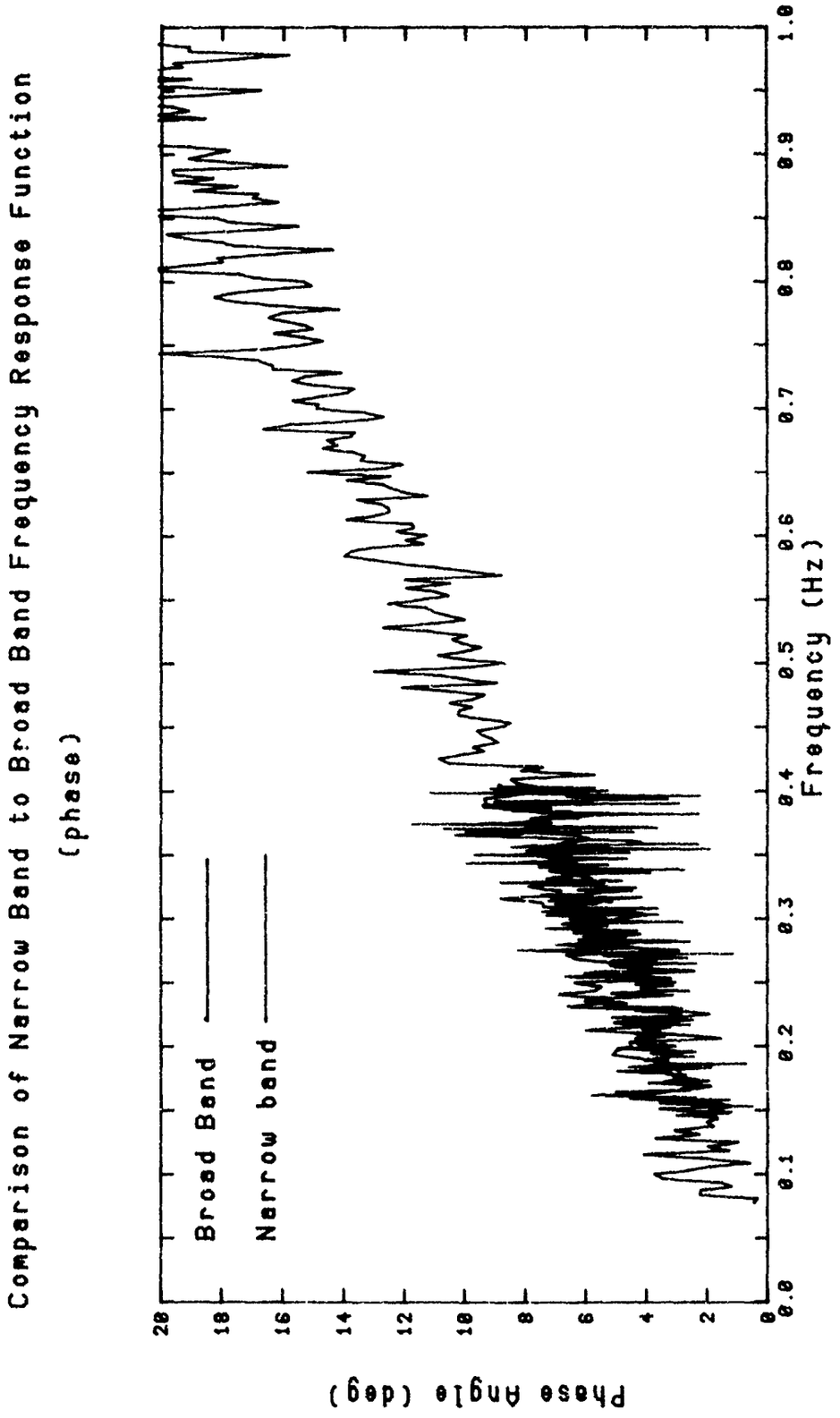
Comparison of Narrow Band to Broad Band Frequency Response Function
(phase)
Broad Band
Narrow band
Phase Angle (deg)
Frequency (Hz)
20
18
16
14
12
10
8
6
4
2
0
0.0
0.1
0.2
0.3
0.4
0.5
0.6
0.7
0.8
0.9
1.0

Figure 9

Graph of Lift Coefficient versus Achieved Hydroplane Angle

(each dot represents one data point from a time history of 4096 data points)

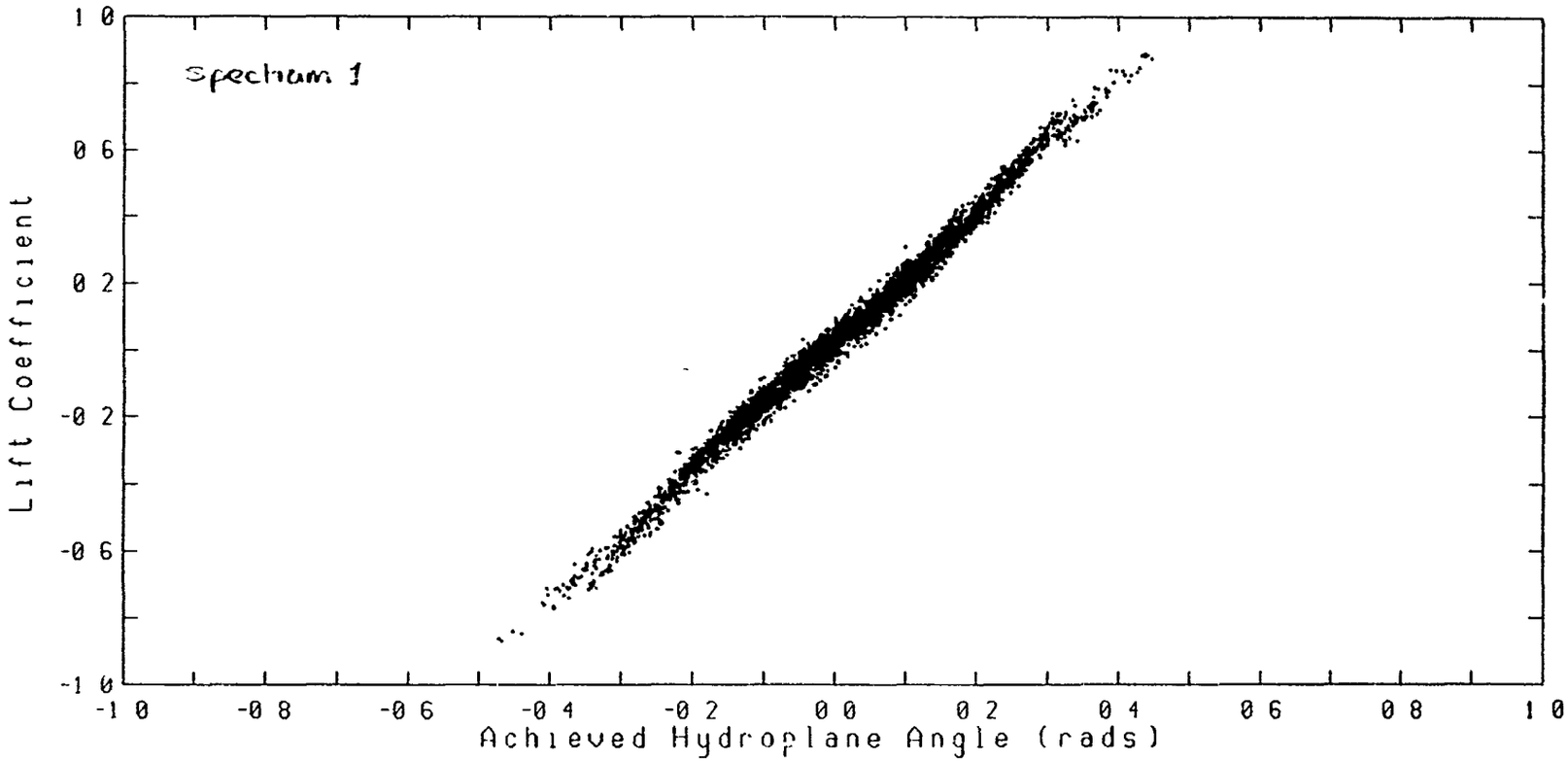

Figure 10

LCRANG 1A

Graph of Lift Coefficient versus Achieved Hydroplane Angle

(each dot represents one data point from a time history of 4096 data points))

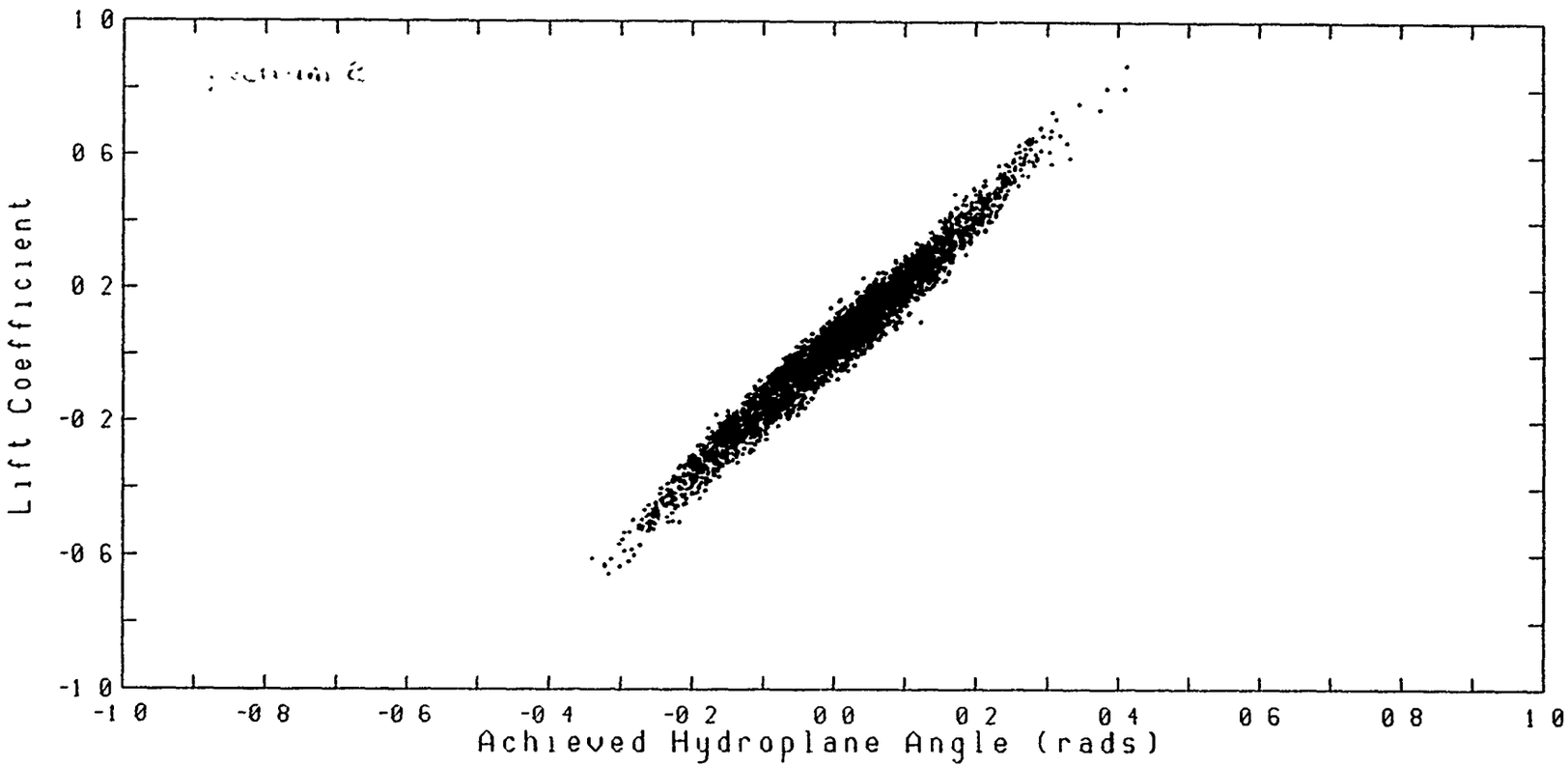

Figure 11

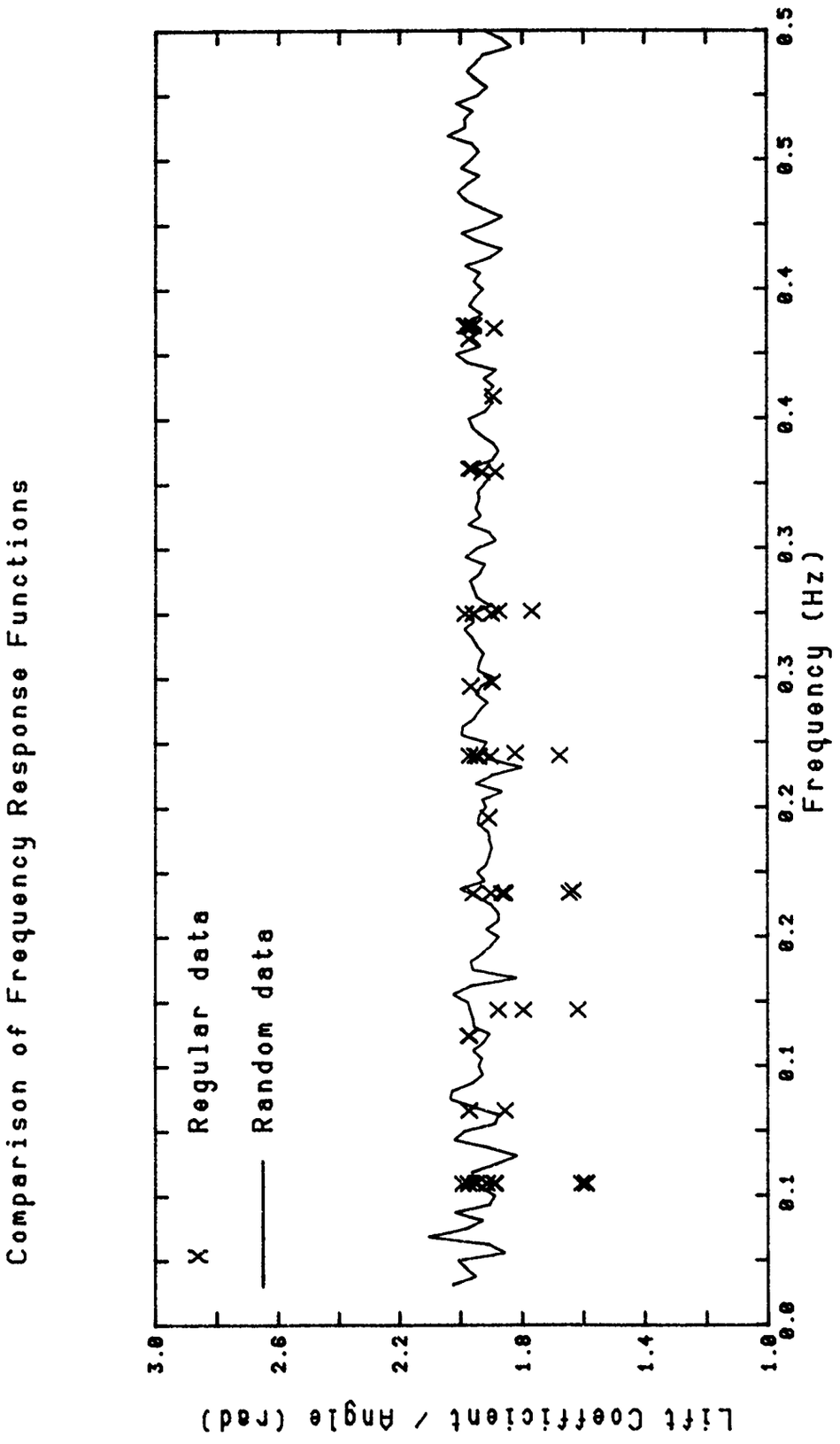
Comparison of Frequency Response Functions
Regular data
Random data
Lift Coefficient / Angle (rad)
Frequency (Hz)
3.0
2.6
2.2
1.8
1.4
1.0
0.0
0.1
0.2
0.3
0.4
0.5

Figure 12

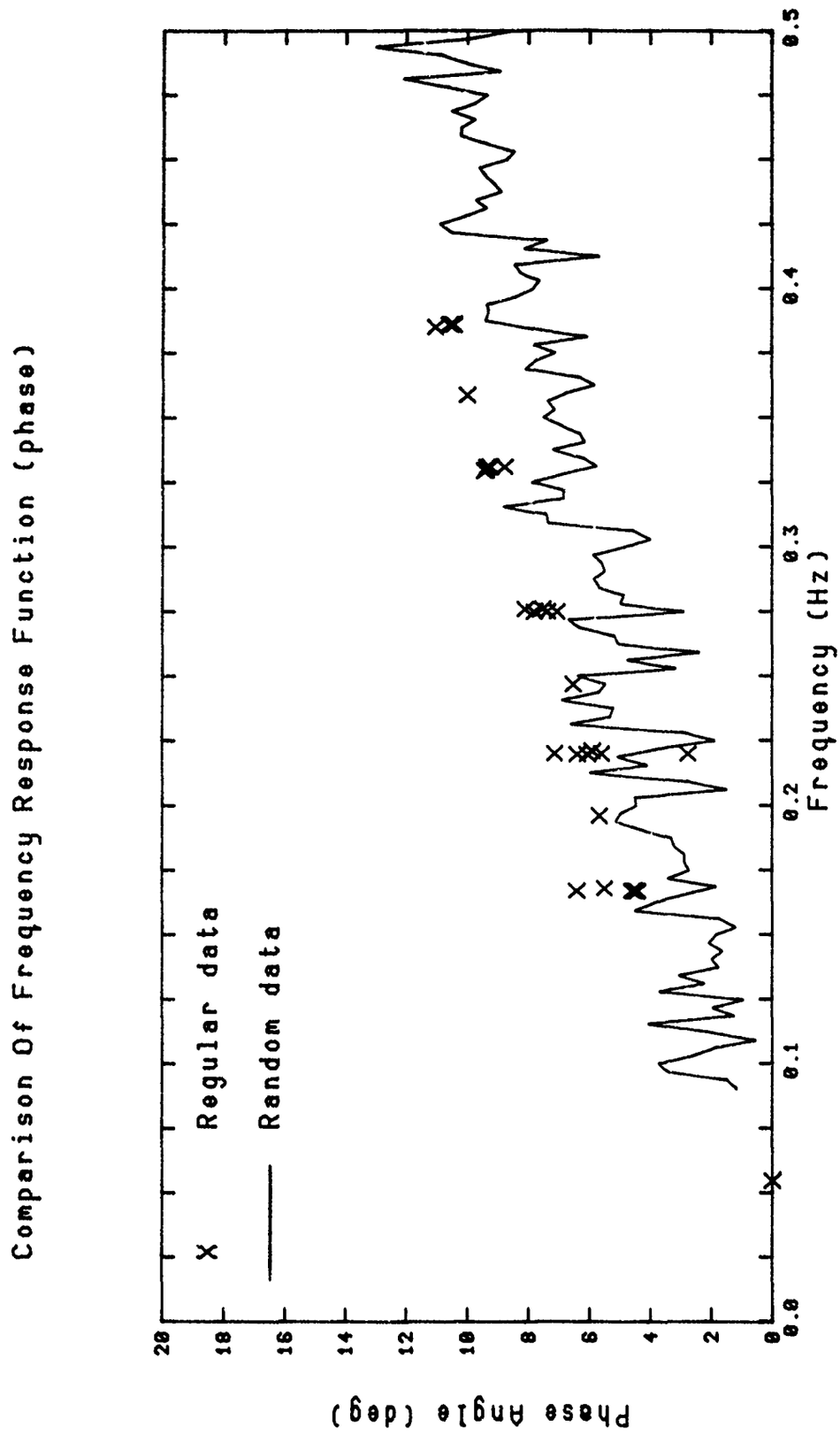
Comparison Of Frequency Response Function (phase)
Regular data
Random data
Phase Angle (deg)
Frequency (Hz)
20
18
16
14
12
10
8
6
4
2
0
0.0
0.1
0.2
0.3
0.4
0.5

Figure 13

Comparison of Steady-state to Dynamic Measurements

For Points Where Angular Velocity and Acceleration are Zero

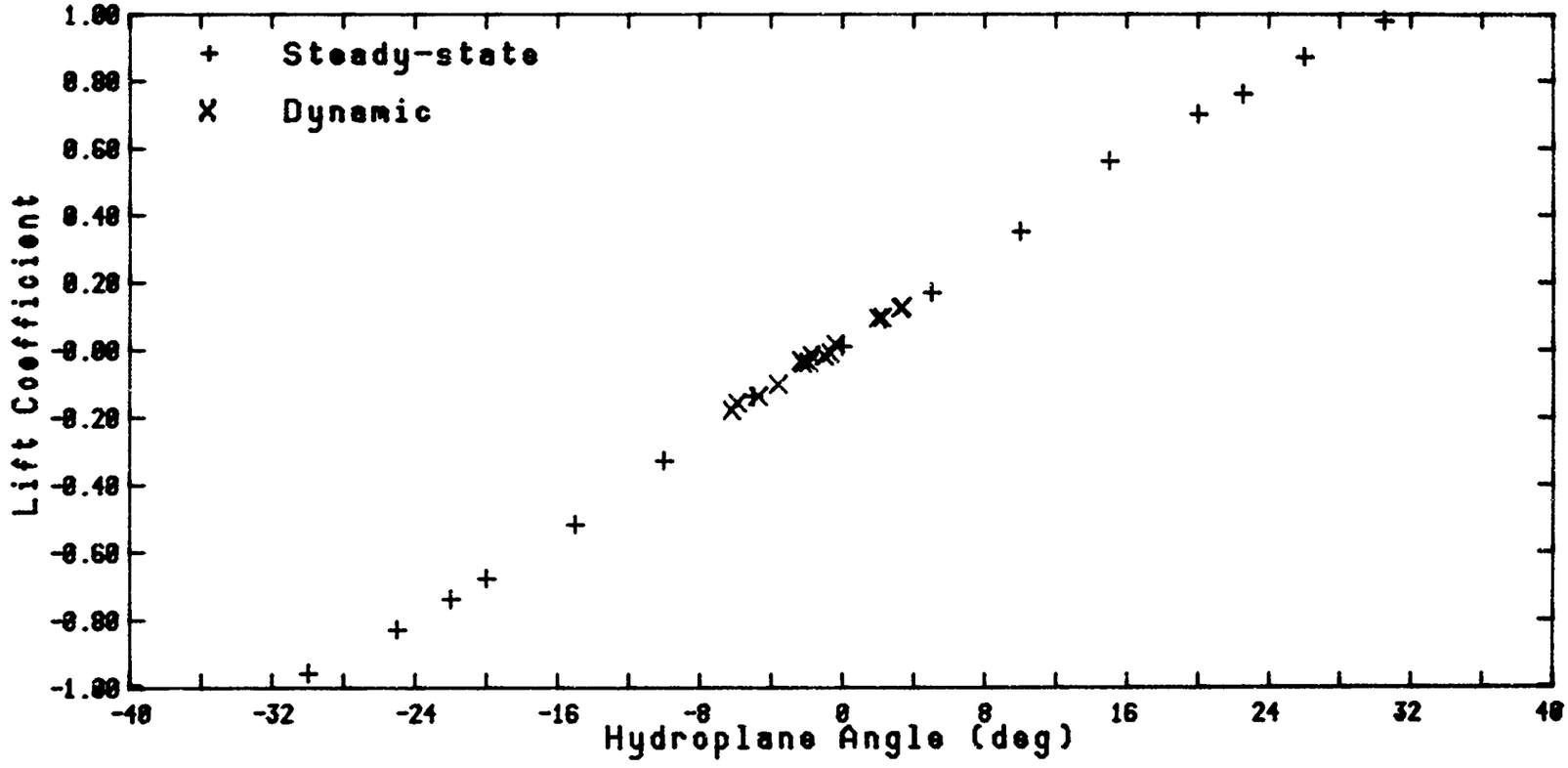

Figure 14

BW.DAC
MJS.DAC

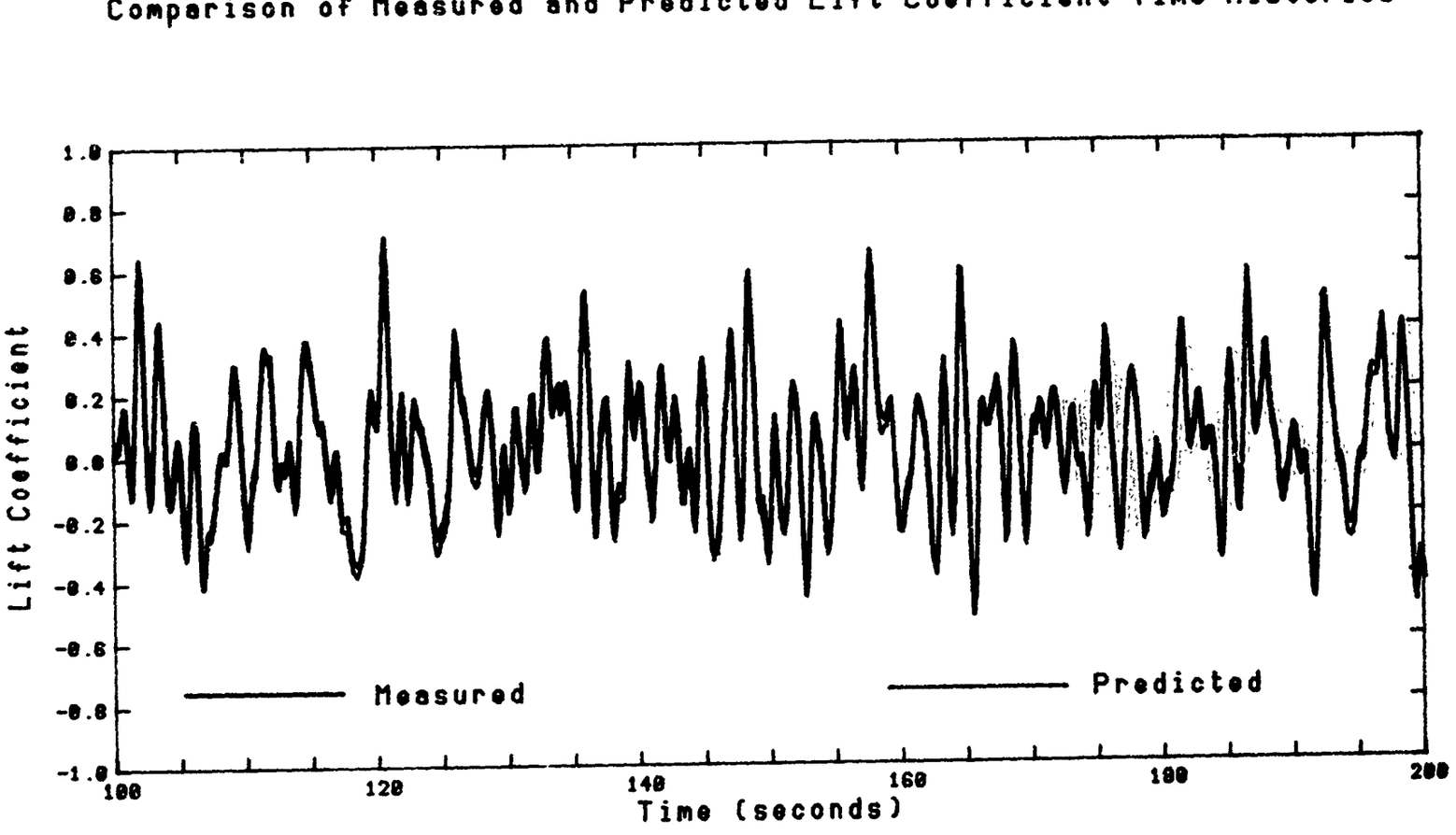
Comparison of Measured and Predicted Lift Coefficient Time Histories
Lift Coefficient
1.0
0.8
0.6
0.4
0.2
0.0
-0.2
-0.4
-0.6
-0.8
-1.0
100
120
140
160
180
200
Time (seconds)
Measured
Predicted

Figure 15

Graph of Lift Coefficient versus Hydroplane Angle
When Angular Velocity and Angular Acceleration are Zero

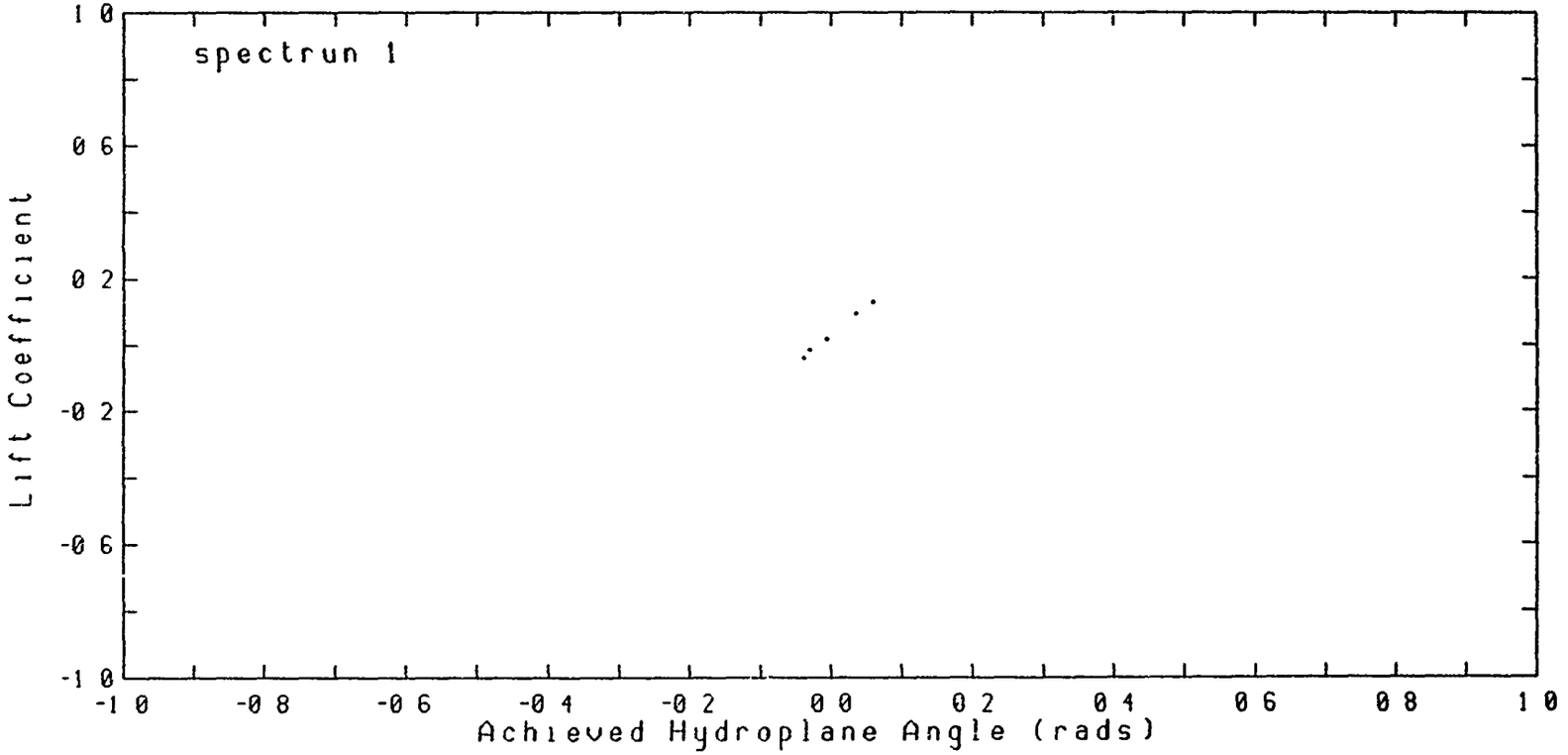

Figure 16

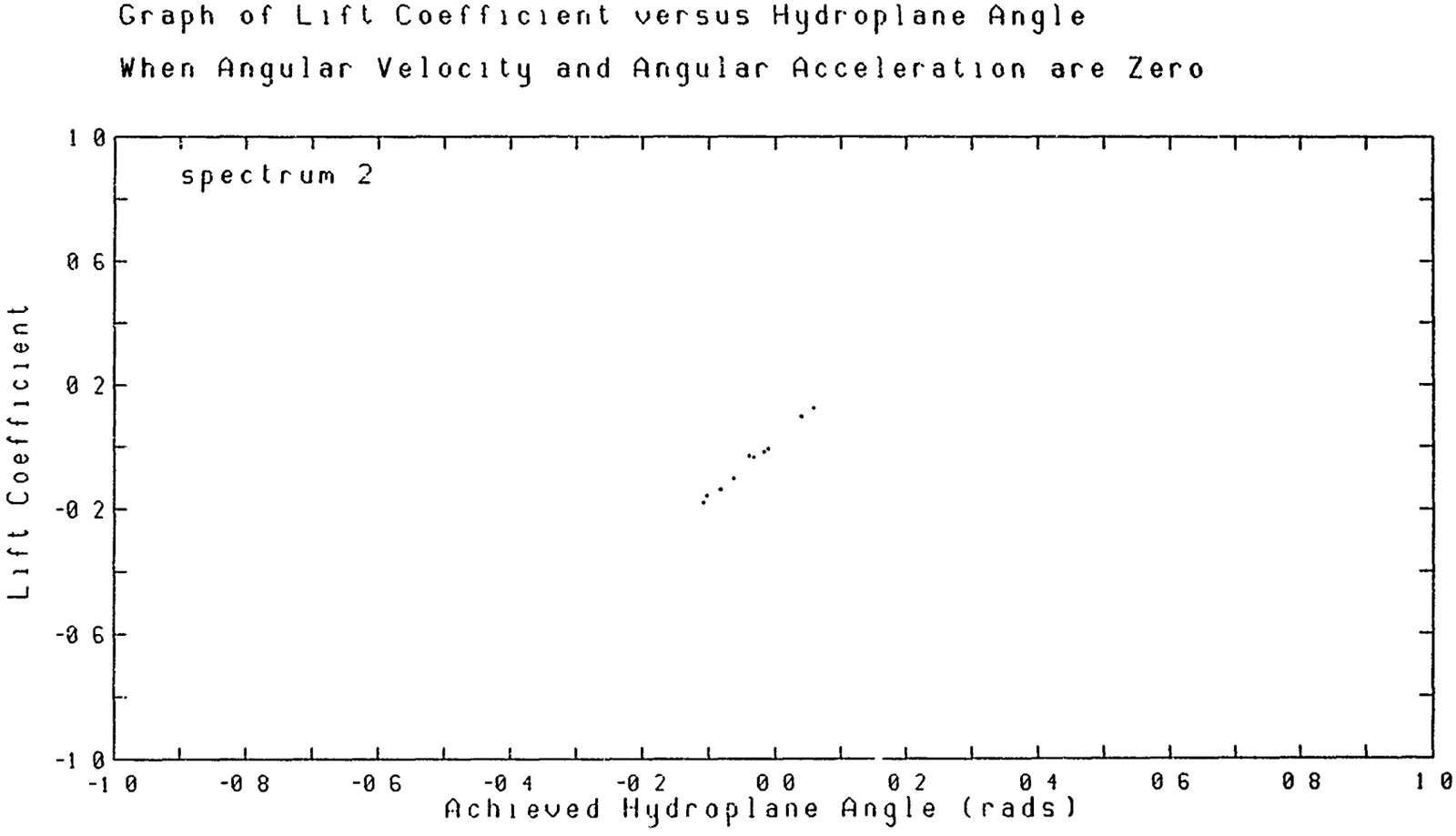
Graph of Lift Coefficient versus Hydroplane Angle
When Angular Velocity and Angular Acceleration are Zero
spectrum 2
Lift Coefficient
1 0
0 6
0 2
-0 2
-0 6
-1 0
-1 0
-0 8
-0 6
-0 4
-0 2
0 0
0 2
0 4
0 6
0 8
1 0
Achieved Hydroplane Angle (rads)

Figure 17

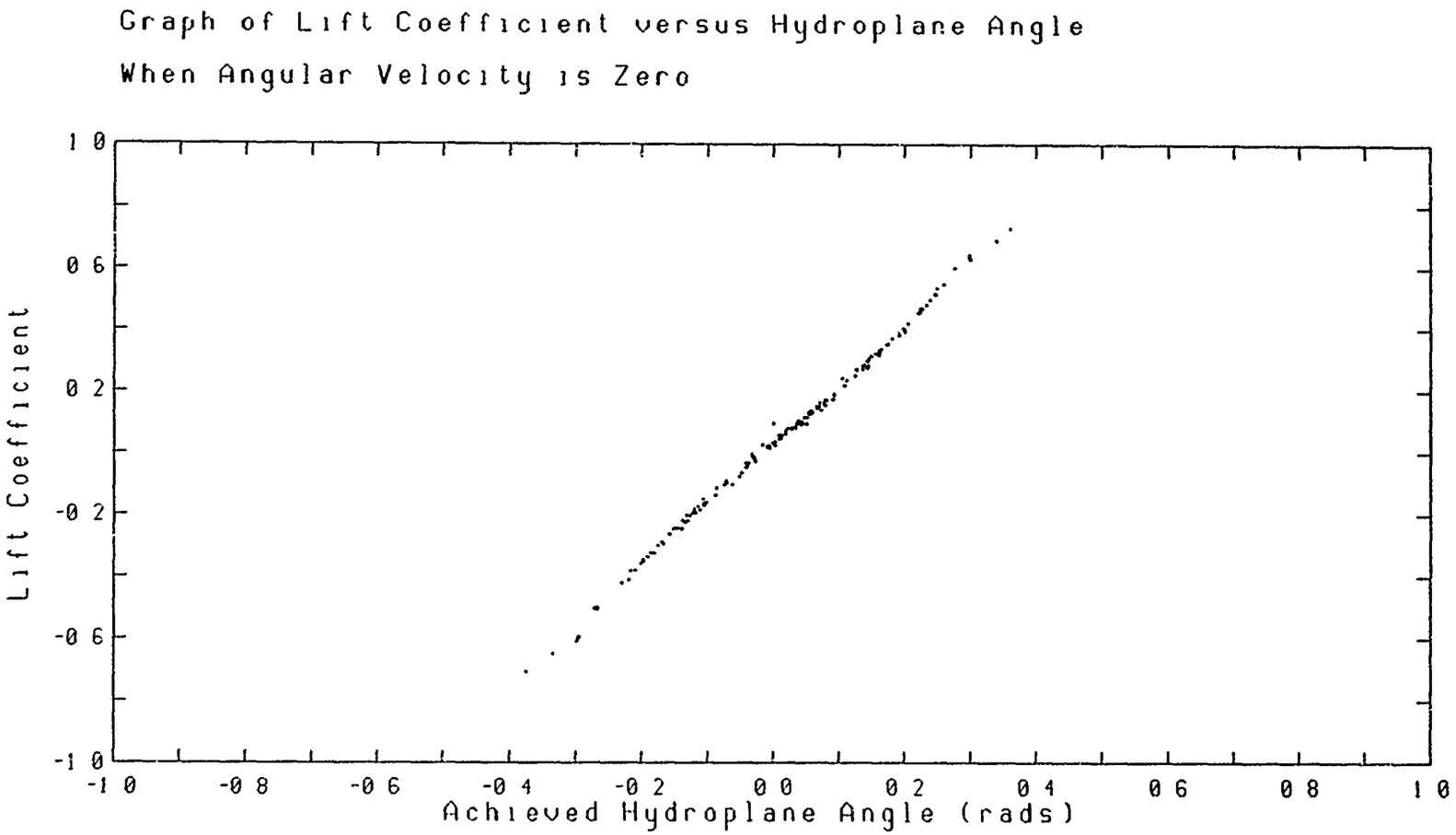

Figure 18

ZEPOV 14

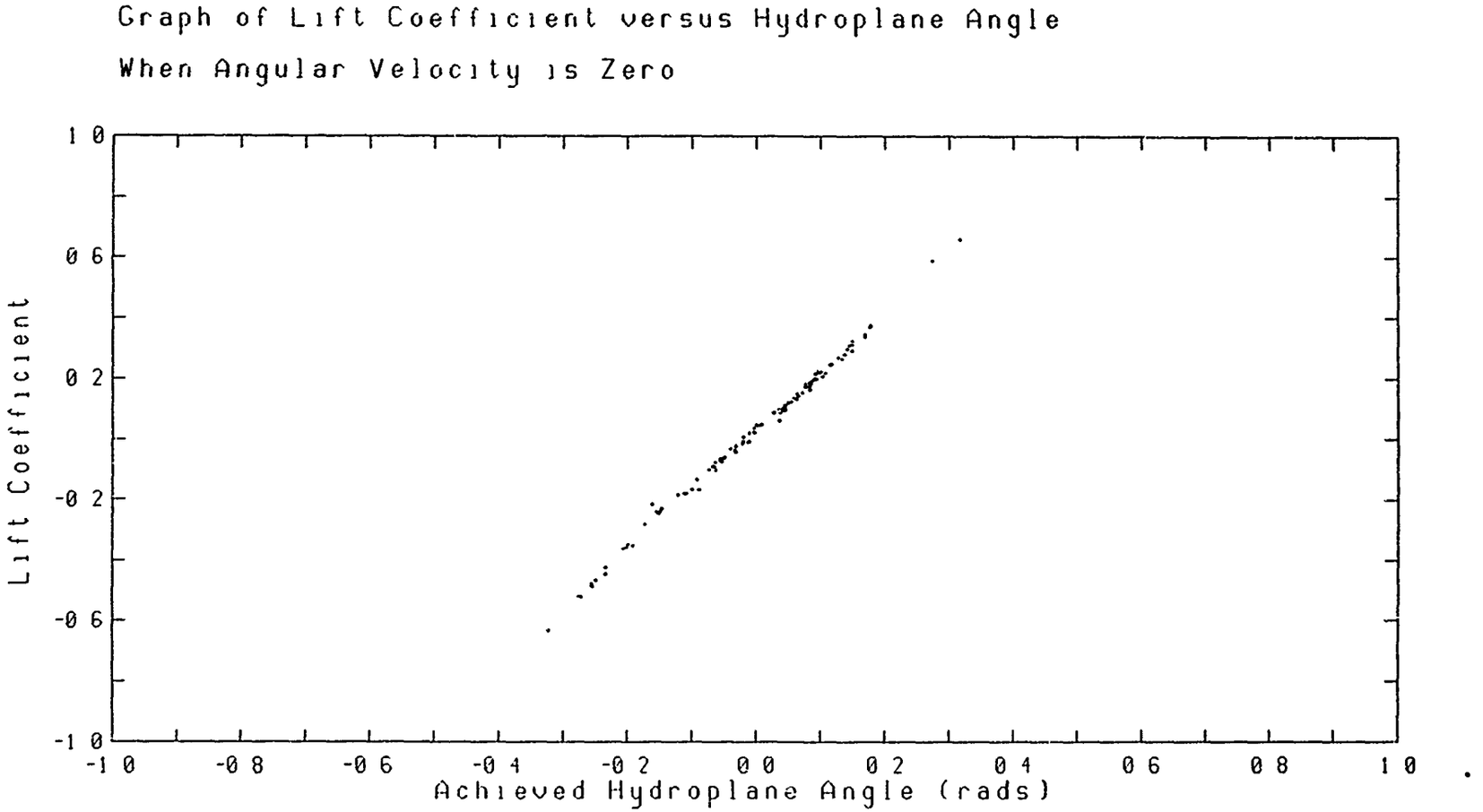
Graph of Lift Coefficient versus Hydroplane Angle
When Angular Velocity is Zero
Lift Coefficient
1 0
0 6
0 2
-0 2
-0 6
-1 0
-1 0
-0 8
-0 6
-0 4
-0 2
0 0
0 2
0 4
0 6
0 8
1 0
Achieved Hydroplane Angle (rads)

Figure 19

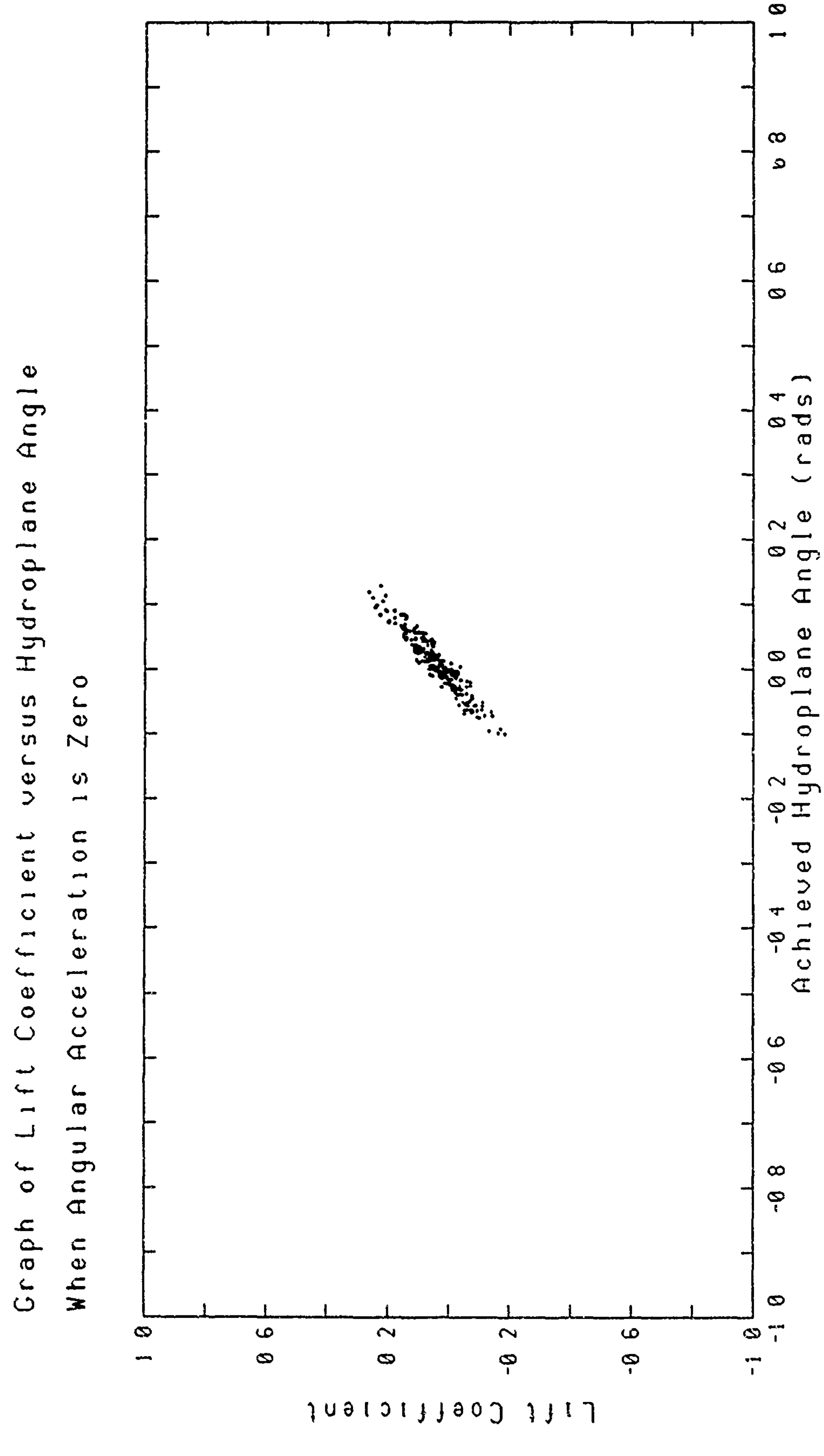

Graph of Lift Coefficient versus Hydroplane Angle
When Angular Acceleration is Zero
Achieved Hydroplane Angle (rads)
Lift Coefficient
1 0
0 8
0 6
0 4
0 2
0 0
-0 2
-0 4
-0 6
-0 8
-1 0

Figure 20

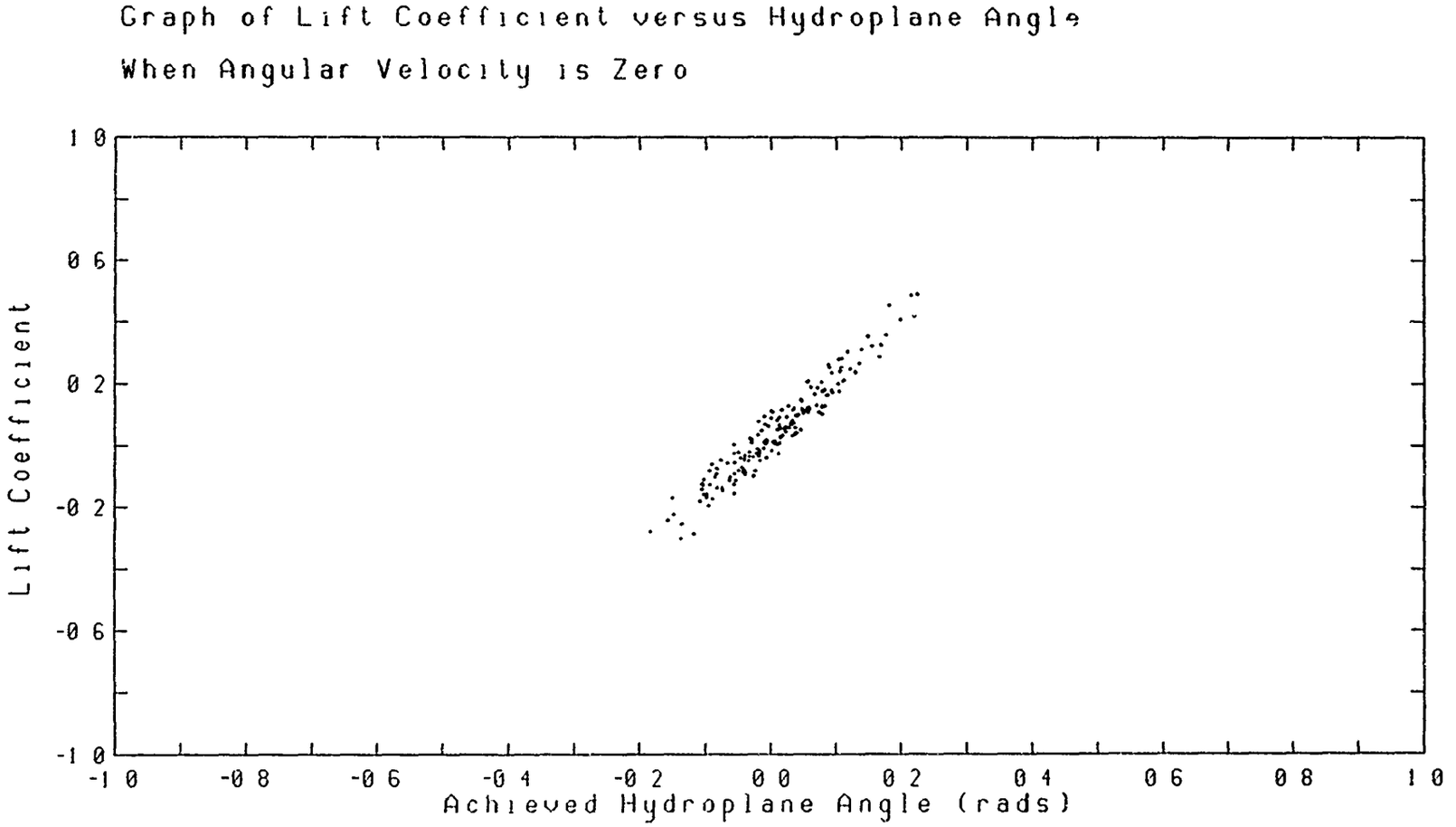
Graph of Lift Coefficient versus Hydroplane Angle
When Angular Velocity is Zero
Lift Coefficient
1 0
0 6
0 2
-0 2
-0 6
-1 0
-1 0
-0 8
-0 6
-0 4
-0 2
0 0
0 2
0 4
0 6
0 8
1 0
Achieved Hydroplane Angle (rads)

Figure 21

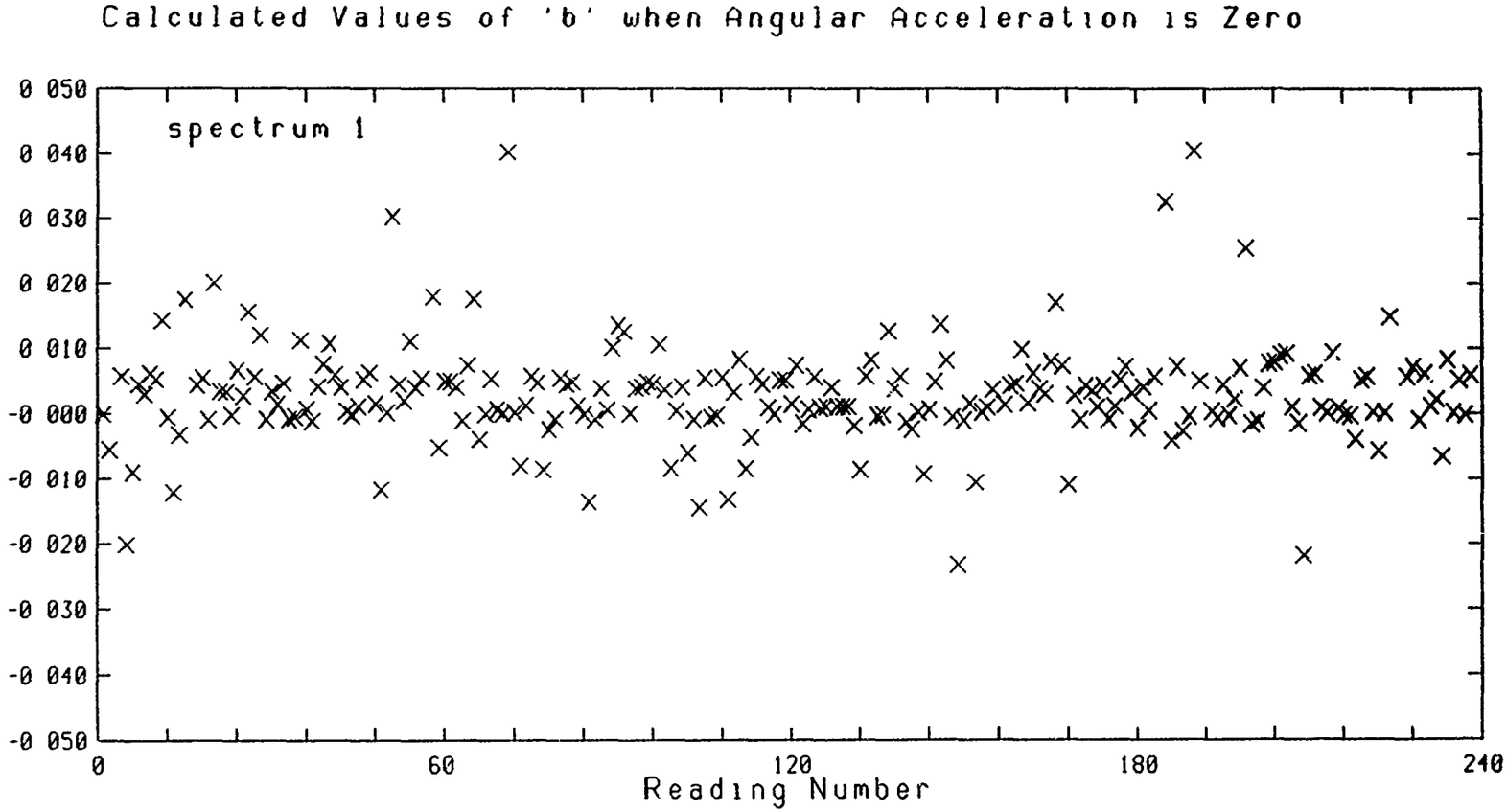
Calculated Values of 'b' when Angular Acceleration is Zero
spectrum 1
0 050
0 040
0 030
0 020
0 010
-0 000
-0 010
-0 020
-0 030
-0 040
-0 050
0
60
120
180
240
Reading Number

Figure 22

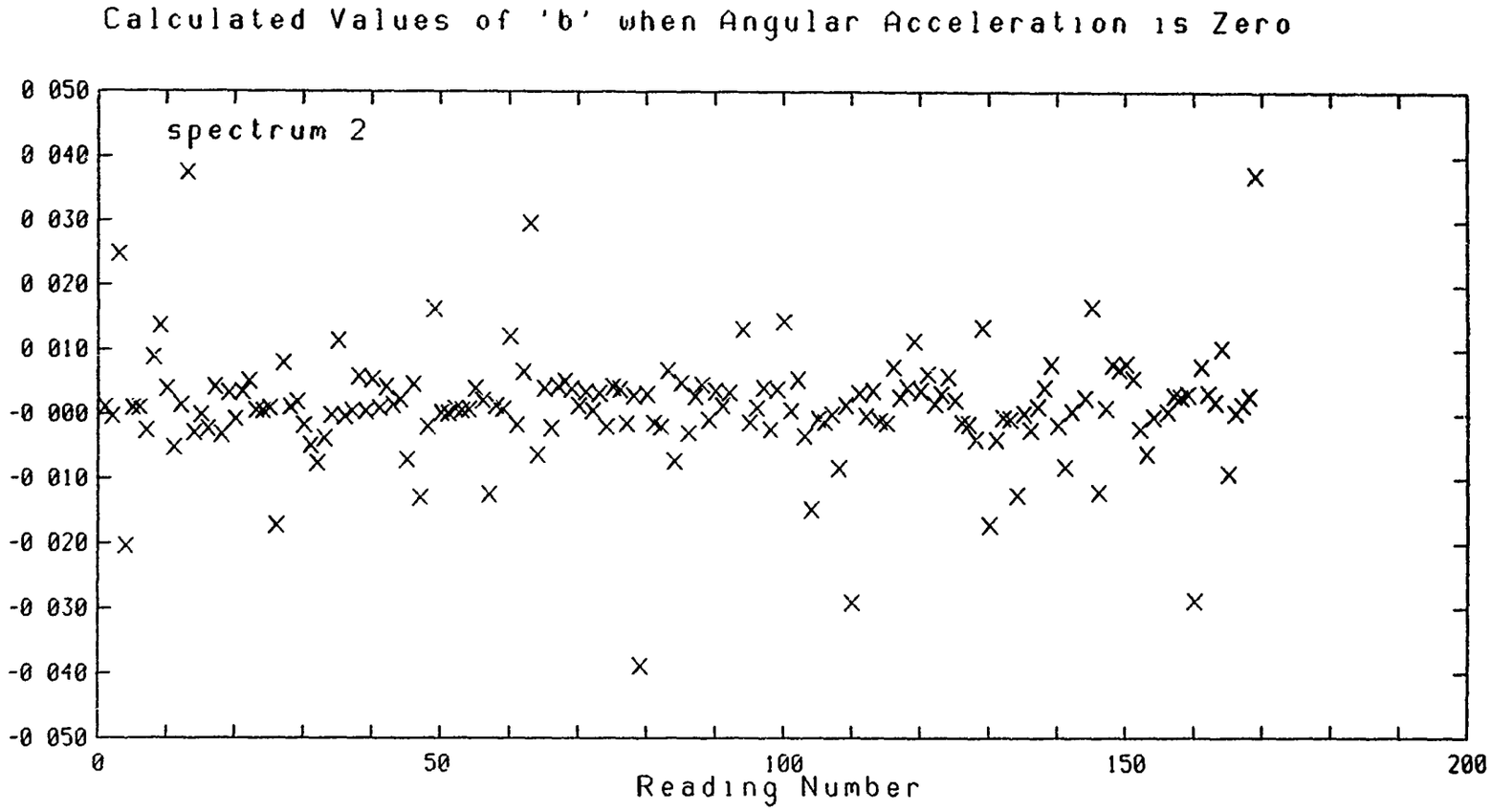
Calculated Values of 'b' when Angular Acceleration is Zero
spectrum 2
0 050
0 040
0 030
0 020
0 010
-0 000
-0 010
-0 020
-0 030
-0 040
-0 050
0
50
100
150
200
Reading Number

Figure 23

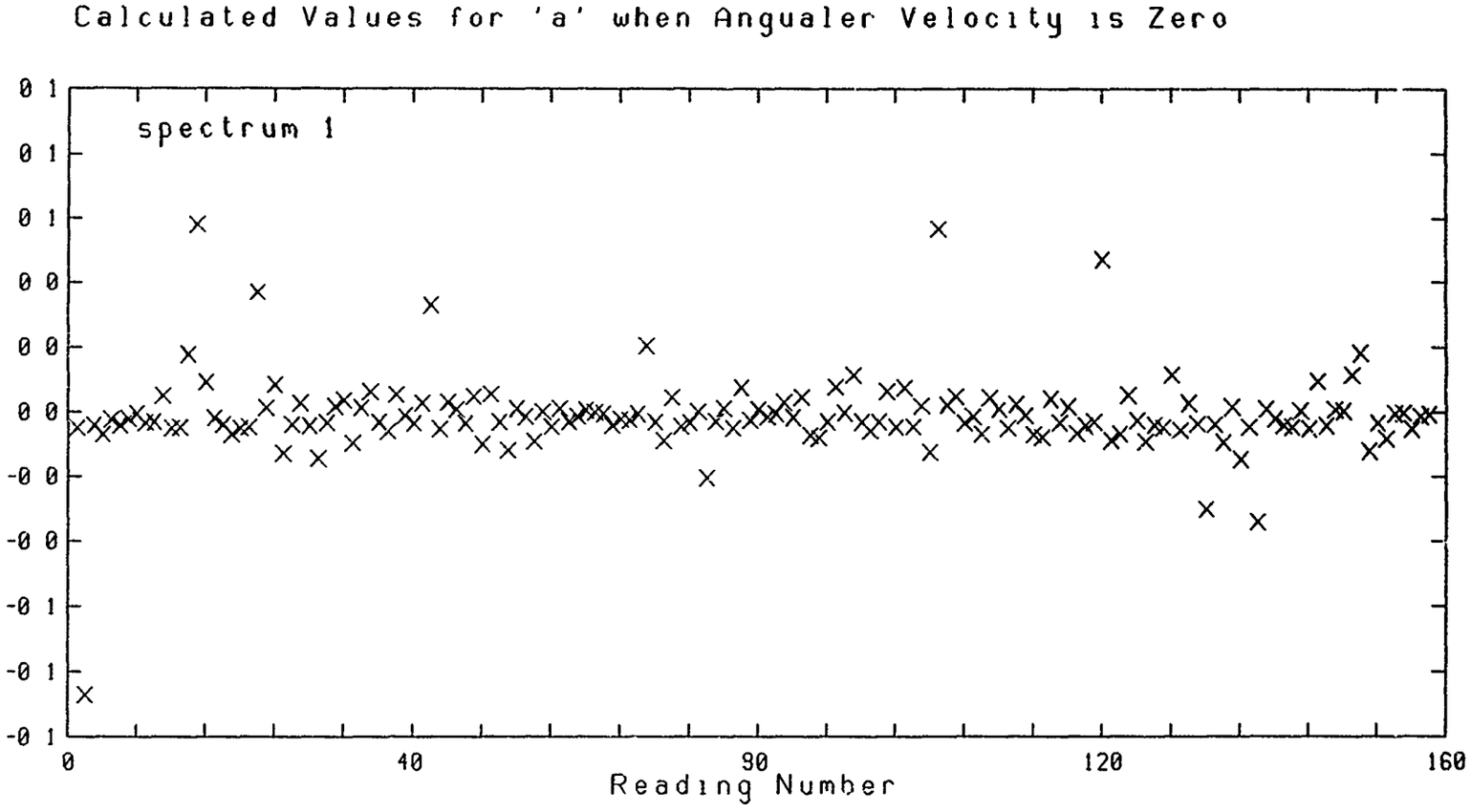
Calculated Values for 'a' when Angualer Velocity is Zero
spectrum 1
0 1
0 1
0 1
0 0
0 0
0 0
-0 0
-0 0
-0 1
-0 1
-0 1
0
40
80
120
160
Reading Number

Figure 24

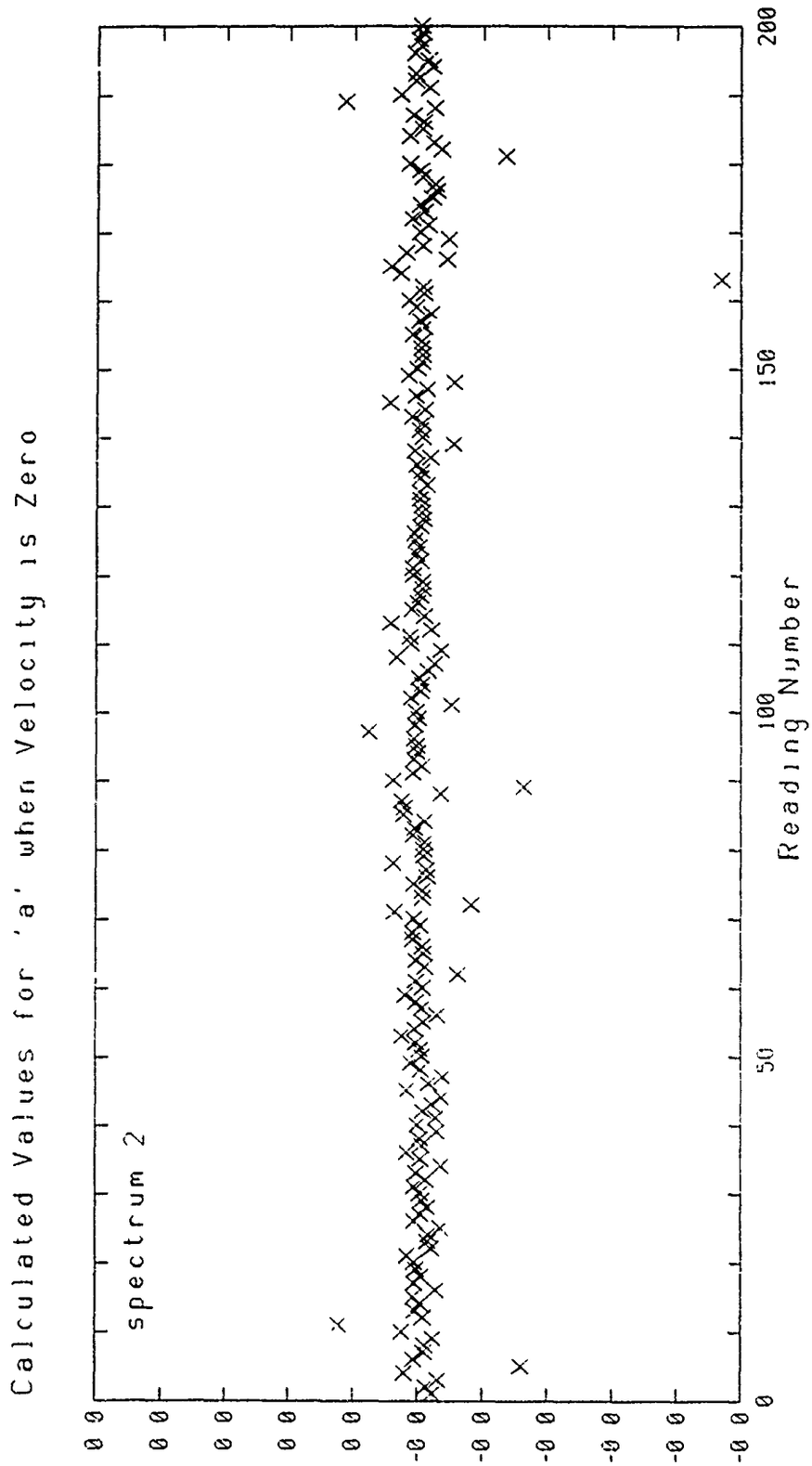
Calculated Values for 'a' when Velocity is Zero
spectrum 2
0.0
0.0
0.0
0.0
0.0
-0.0
-0.0
-0.0
-0.0
-0.0
0
50
100
150
200
Reading Number

Figure 25

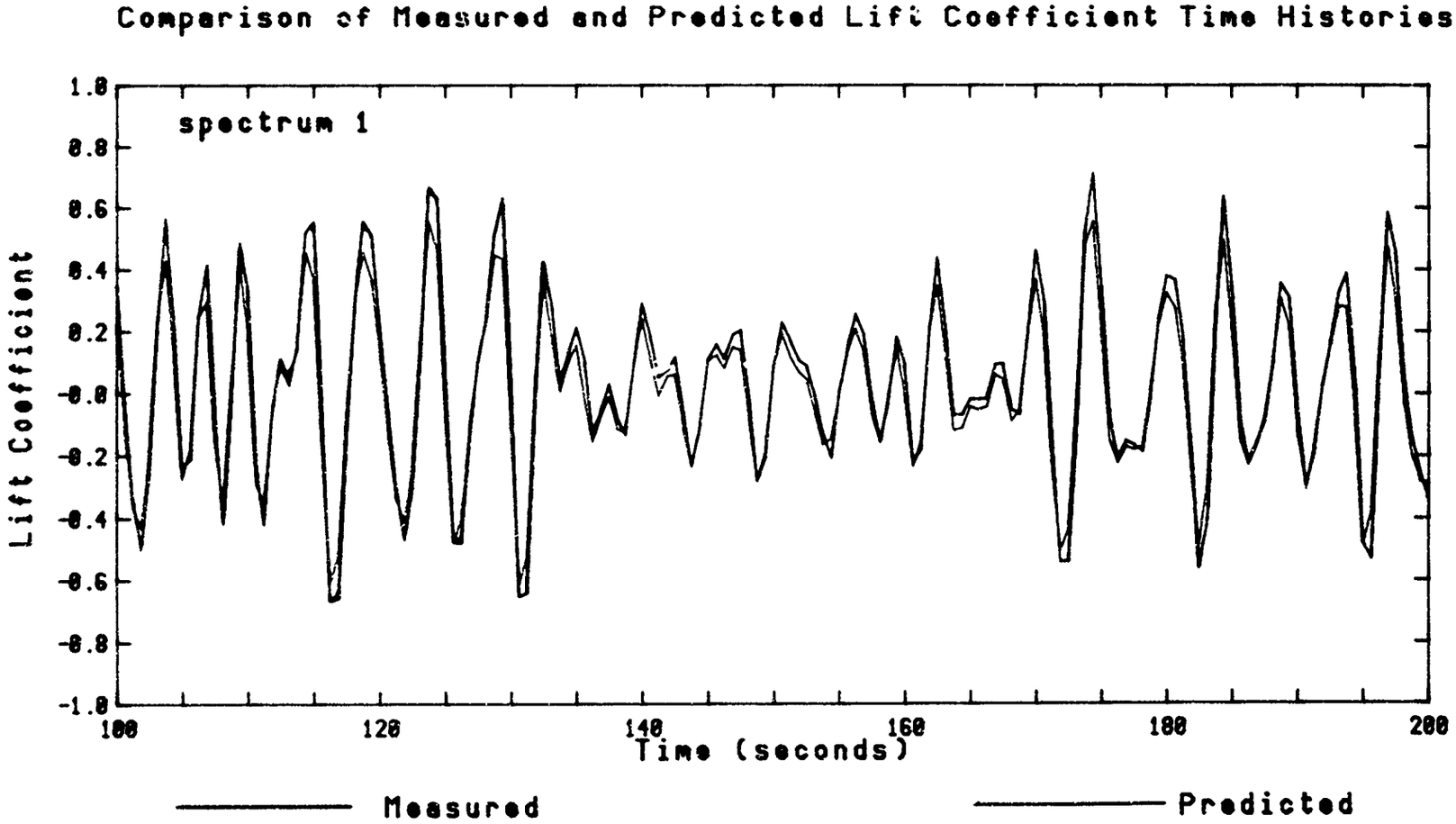

Figure 36

LCRANG.1A
CL.1A

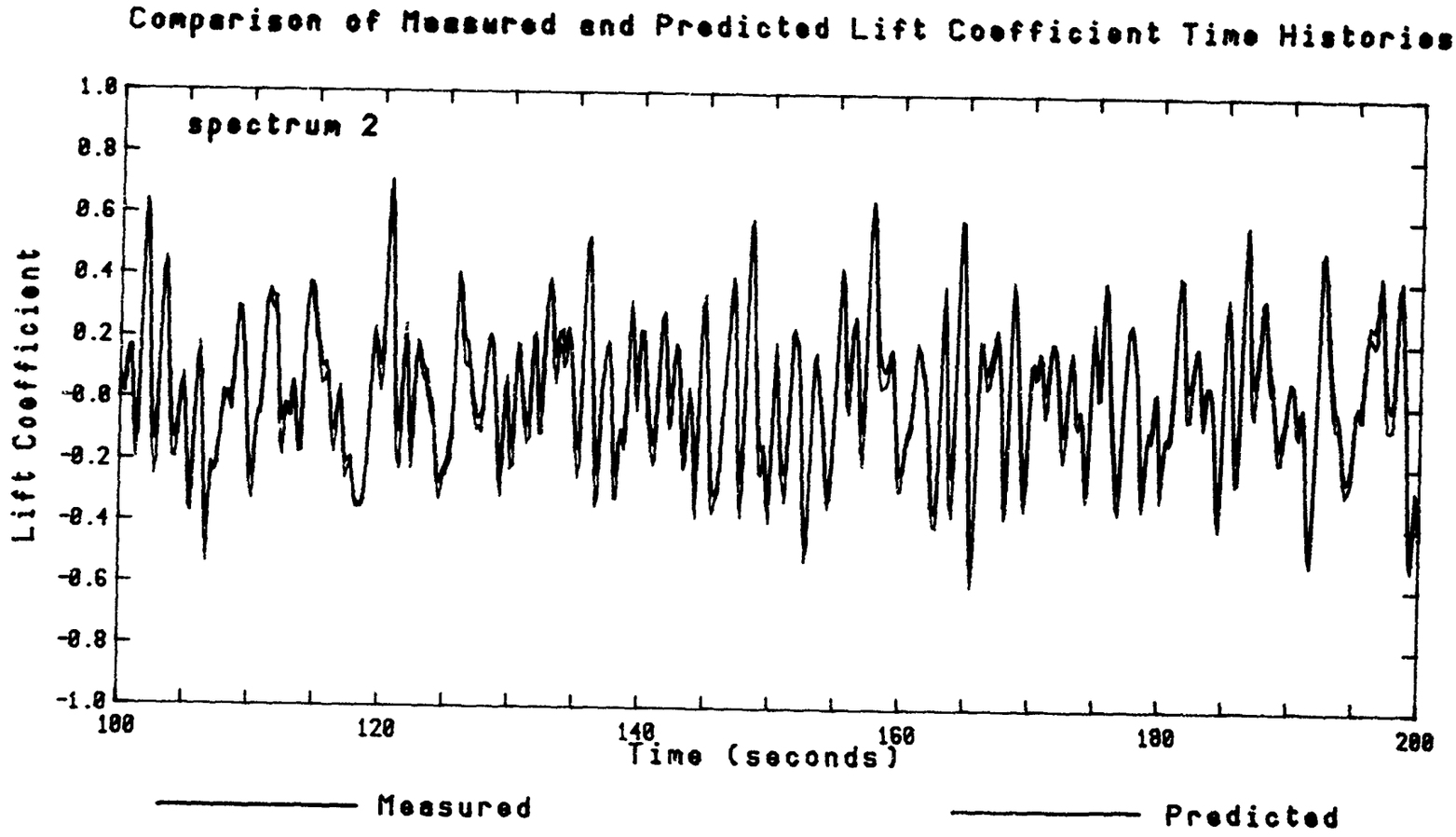

Figure 27

LCRANG.2A
CL.2A

Figure 38

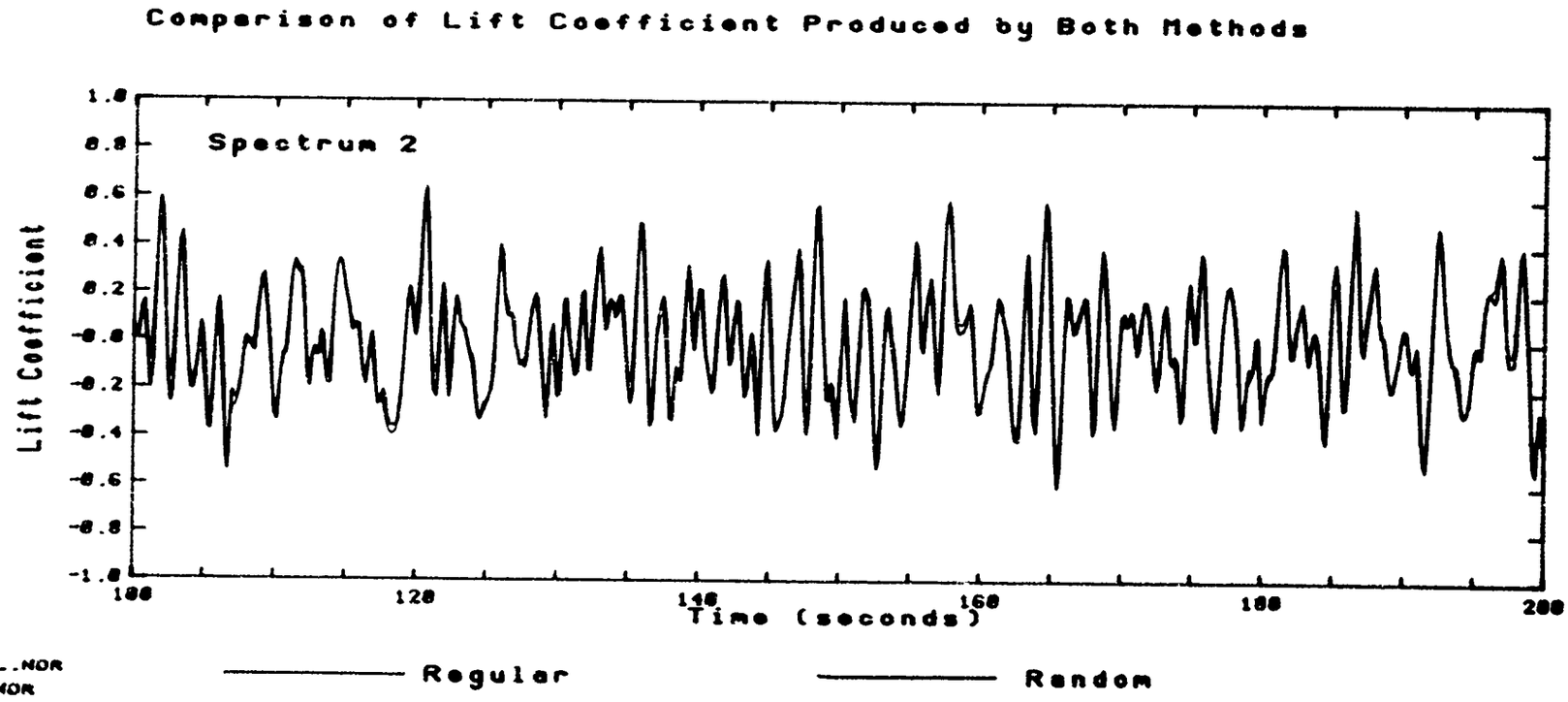
Comparison of Lift Coefficient Produced by Both Methods
Spectrum 2
Lift Coefficient
1.0
0.8
0.6
0.4
0.2
0.0
-0.2
-0.4
-0.6
-0.8
-1.0
100
120
140
160
180
200
Time (seconds)
BWCL.NOR
CL.NOR
Regular
Random

Distribution

Copy Numbers	1-2	ADNA/SM NA112
	3	Staff Officer (C) BNS
	4-8	US Navy Technical Liaison Officer
	9	Managing Director Maritime Division
	10	Author
	11-40	DRIC
	41-42	Library DRA Maritime Division, Portsdown
	43-44	Library DRA Maritime Division, Portland
	45	CS(R)2e (Navy) Hayes
	46-52	Library DRA Maritime Division, Haslar